RADIOASTRON USER HANDBOOK

Prepared by the RadioAstron Science and Technical Operations Group
Version 2.7; 17 December 2015

Contents

1 Introduction **3**

1.1 Basic information . . . 3

1.2 Main performance parameters of RadioAstron . . . 4

2 RadioAstron Space Segment **4**

2.1 Spacecraft design . . . 4

2.1.1 The Onboard Command and Measuring System (OCMS) . . . 9

2.1.2 The Spacecraft Onboard Control System (OCS) . . . 9

2.2 Scientific payload . . . 10

2.2.1 Space Radio Telescope (antenna) . . . 10

2.2.2 The Feed System . . . 11

2.2.3 The Receivers . . . 11

2.2.4 The Formatter . . . 11

2.2.5 High-Data-Rate Communication radio links (HDRC) . . . 12

2.2.6 The System of Frequency Synthesis (SFS) . . . 12

2.2.7 The Control System (CS) . . . 13

2.3 RadioAstron orbit . . . 13

2.3.1 Initial orbit elements and their evolution . . . 13

2.3.2 Orbit Measurement (OM), prediction, and reconstruction . . . 16

2.4 Operational constraints . . . 17

2.4.1 Constraints connected with SC service systems . . . 17

2.4.2 Constraints connected with the science payload . . . 19

2.5 Pointing offsets and gain measurements . . . 19

2.6 Calibration . . . 20

2.6.1 Noise calibration . . . 20

2.6.2 Pulse calibration . . . 20

3 RadioAstron Ground Segment and Operations **20**

3.1 Tracking stations . . . 20

3.2 Ground radio telescopes . . . 21

3.3 Data recording . . . 21

3.4 Data correlation . . . 21

3.4.1 ASC correlator . . . 21

3.4.2 DiFX correlator . . . 22

3.4.3 SFXC correlator 22
3.5 Satellite operations and experiment scheduling 22
3.6 Observational modes and procedures 23
3.7 Science access 23

4 Observations with RadioAstron 24
4.1 The Frequency setup 24
4.1.1 K-band observing and MFS 26
4.2 Resolution 26
4.3 System sensitivity 26
4.4 Experiment preparation 27
4.5 Observing strategy and imaging 27
4.5.1 All-sky (u,v)-plots 27
4.5.2 Examples of observing strategies 30
4.5.3 Imaging capabilities 30
4.6 Post-correlation data processing 31

A Document abbreviations 34

B Abbreviations used in the Diagrams 35

1 Introduction

This Handbook describes the design guidelines and the constraints that govern the use of all systems of the RadioAstron mission, and serves as an observer aid on the technical and operational issues related to generating an observing proposal.

The Handbook will be updated as needed and is available at the RadioAstron web site. We encourage all readers and users to provide comments.

1.1 Basic information

The RadioAstron Project was initiated by the Astro Space Center (ASC) of the P.N. Lebedev Physical Institute of the Russian Academy of Science.

The RadioAstron project is an international collaborative mission centered on the 10-m space radio telescope, Spektr-R, which is in an elliptical orbit around the Earth. The aim of the mission is to use the space telescope for radio astronomical observations using VLBI (Very Long Baseline Interferometry) techniques in conjunction with ground-based VLBI networks located in Australia, Chile, China, Europe, India, Japan, Korea, Mexico, Russia, South Africa, Ukraine, and the USA.

The orbit of the RadioAstron satellite evolves with time and has an apogee height between 270,000 and 370,000 km, a perigee between 7,000 and 80,000 km, a period of 8 to 9 days, and an initial inclination of 51°. RadioAstron operates at the standard radio astronomical wavelengths of 1.19–1.63 cm (K-band), 6.2 cm (C-band), 18 cm (L-band), and 92 cm (P-band). Space-Ground VLBI observations using RadioAstron provide morphological information on galactic and extragalactic radio sources with fringe size of 7 μas at the highest frequency and the longest baselines. The spacecraft's operational lifetime is five years.

The Spektr-R spacecraft was launched from Baikonur on July 18, 2011, and its on-board 10-metre SRT antenna was successfully unfolded on July 23, 2011. The telescope then underwent detailed in-orbit checkout (IOC) testing. The on-board hydrogen maser was switched on, orbital parameters started to be routinely determined using Doppler tracking and laser ranging, the radiometers were turned on and system temperatures were measured in all four bands (P, L, C, and K). Information on the RadioAstron status is updated regularly in RadioAstron Newsletters[1] and a list of RadioAstron publications[2].

International contributions: During the long period of project development, institutes from other countries have made notable contributions to the RadioAstron Project. The low-noise amplifier (LNA) for the 92-cm (P-band) receiver operating at 327 MHz was built in India by NCRA. The 18-cm (L-band) receiver operating at 1665 MHz was developed in Australia by CSIRO. The initial 6.2-cm (C-band) receiver operating at 4830 MHz was developed at ASTRON, the Netherlands, and MPIfR, Germany, on behalf of the European VLBI Consortium (EVN). Finally, the initial 1.35-cm (K-band) receiver operating at 22 GHz was provided by the Helsinki University of Technology in Finland. Due to aging issues, the C- and K-band receivers were replaced before launch by new models developed in Russia. The new K-band receiver contains an LNA provided by the NRAO, USA, and can operate in frequency switching mode in the range of 18.392–25.112 GHz. The original receivers were extensively used in system development tests, and particularly in the astronomical tests of the complete engineering complex of the SRT in Pushchino in 2004. In addition, the European Space Agency (ESA) conducted detailed tests of the SRT antenna petals in the vacuum chamber in Noordwijk. These test were essential for the final development of the RadioAstron project. ESA has also provided funding for

[1] `http://www.asc.rssi.ru/radioastron/news/news.html`

[2] `http://www.asc.rssi.ru/radioastron/publications/publ.html`

the development of the on-board Rubidium frequency standard, which has been manufactured by the Neuchatel Astronomical Observatory in Switzerland. The S2 recording and playback facilities, which helped in the development of the RadioAstron Data Recorder (RDR) and ASC software correlator, were provided by the Canadian Space Agency and York University in Toronto, Canada.

During the fringe search period of the IOC tests many observatories committed necessary observing time for the mission, including NAIC with the 300-m telescope in Arecibo, NRAO with the GBT, MPIfR with the 100-m Effelsberg radio telescope, ASTRON with the WSRT, IRA (Italy) with Medicina and Noto, JAXA (ISAS) with the Usuda 64-m telescope, Jodrell Bank, Evpatoria 70-m dish of Ukranian Space Agency, three 32-m telescopes (Badary, Svetloe and Zelenchuk) of the Institute of Applied Astronomy in Saint Petersburg, and the Yebes 40-m telescope.

1.2 Main performance parameters of RadioAstron

The main performance metrics of the Space Radio Telescope in flight are shown in Table 1. See section 4 for details.

Table 1: Basic performance of RadioAstron

Observing Bands (cm)	Frequency range (MHz)	Bandwidth per polarization (MHz)	Smallest spacing (μas)	SEFD (kJy) LCP;RCP	Gain (mK Jy^{-1})	1σ baseline sens. (mJy) LCP; RCP
92 (P)	316 – 332	1×16	530	13.3; 13.5	11	14; 14
18 (L)	1636 – 1692	2×16	100	2.76; 2.93	15	3; 3
6 (C)	4804 – 4860	2×16	35	11.6; —	13	5; —
1.3 (K)	18372 – 25132	2×16	7	46.7; 36.8	3	17; 15

K-band observing can be done at one of the eight central frequencies: 18392, 19352, 20312, 21272, 22232, 23192, 24152, 25112 MHz (with further fine tuning, see section 4.1.1 and Table 4). The fringe spacing is calculated for the longest possible baseline. The one-sigma baseline sensitivity is estimated for the RadioAstron–GBT pair for a 300 s integration time and 16 MHz bandwidth of a single polarization single frequency channel (IF). Image sensitivity is discussed in section 4.5.3.

2 RadioAstron Space Segment

The space segment of the mission is comprised of the RadioAstron satellite hosting a 10-meter parabolic antenna, scientific payload, communication system, and a spacecraft bus. A detailed description of these elements of the satellite is given below.

2.1 Spacecraft design

The RadioAstron satellite consists of a parabolic reflector, a scientific payload located in two containers, the focal container and the instrumentation module, and a “Navigator” service module (bus), which is a standard module used in several other scientific missions. An on-board Hydrogen frequency standard is installed separately. The space radio telescope (SRT) is a deployable parabolic reflector (10-m diameter) made of 27 carbon fiber petals. It has a focal length to diameter ratio, F/D, of 0.43, and an overall RMS surface accuracy ± 0.5 mm. The prime focus concentric feed arrangement

provides the possibility of observing at two frequencies, or two circular polarizations, simultaneously. The observing frequencies are: 0.324, 1.665, 4.830 and 18.392–25.112 GHz. The total satellite mass is 3660 kg, of which 2500 kg is the scientific payload including the SRT, and 1160 kg is the Navigator service module. The satellite was launched from Baikonur by the Zenit-2SB launcher manufactured by the Ukrainian KB-Yuzhnoe company. The satellite's elliptical orbit, with an apogee height of about 320,000 km, was achieved by a Fregat-SB rocket upper stage.

A general overview of the systems of the RadioAstron spacecraft is shown in Figure 1, while Figure 2 presents the general diagram of the on-board scientific complex and Figure 3 — the detailed functional diagram. The service module Navigator consists of the following basic spacecraft subsystems:

- onboard command and measuring system (OCMS)
- onboard control system (OCS)
- telemetry system (TMS)
- power supply system (PSS)
- thermal control system (TCS)
- autonomous electronics module (AE)
- low gain telemetry (TM) antenna and feed system (TMAFS)
- high data rate communication radio link (HDRC)
- up-down phase transfer radio link (UDPTR)
- solar panel Onboard Control System (SPAS)
- orbit correction engines (OCE)

These systems are responsible for keeping the spacecraft operable during periods with radio contact with a ground station and during autonomous operation without direct radio contact.

Operational commands are generated in the Onboard Command and Measuring System (OCMS) during Command & Telemetry Session (CTS) contact and in the Onboard Control System (OCS) for periods without CTS contact, which can be programmed during flight. Operational (observational) programs can be carried out in real-time during a radio contact by means of instructions transmitted from the ground, and in the autonomous mode by instructions stored in the Time-Program System (TPS) that is also part of the OCMS. The basic function of the TPS is that of command-dispatcher for spacecraft systems that are controlled by corresponding TPS-programs. TPS programs are a sequence of macro-instructions and information codes, which produce transmissions of timed Control Code Word (CCW) sequences addressed to any device. The entire memory of the TPS comprises 10K 16-bit words. This software-hardware complex of TPS is designed for:

- generating and transmitting clock frequencies for the vehicle service systems;
- providing the exchange of Control Code Words (CCWs) between the vehicle systems;
- executing fixed (stored in ROM) or flexible (stored in RAM) time-sequence using CCWs for the vehicle systems;
- keeping vehicle time and transmitting time codes to the vehicle service systems;
- recording and storing CCW settings and transmitting them to the vehicle systems.

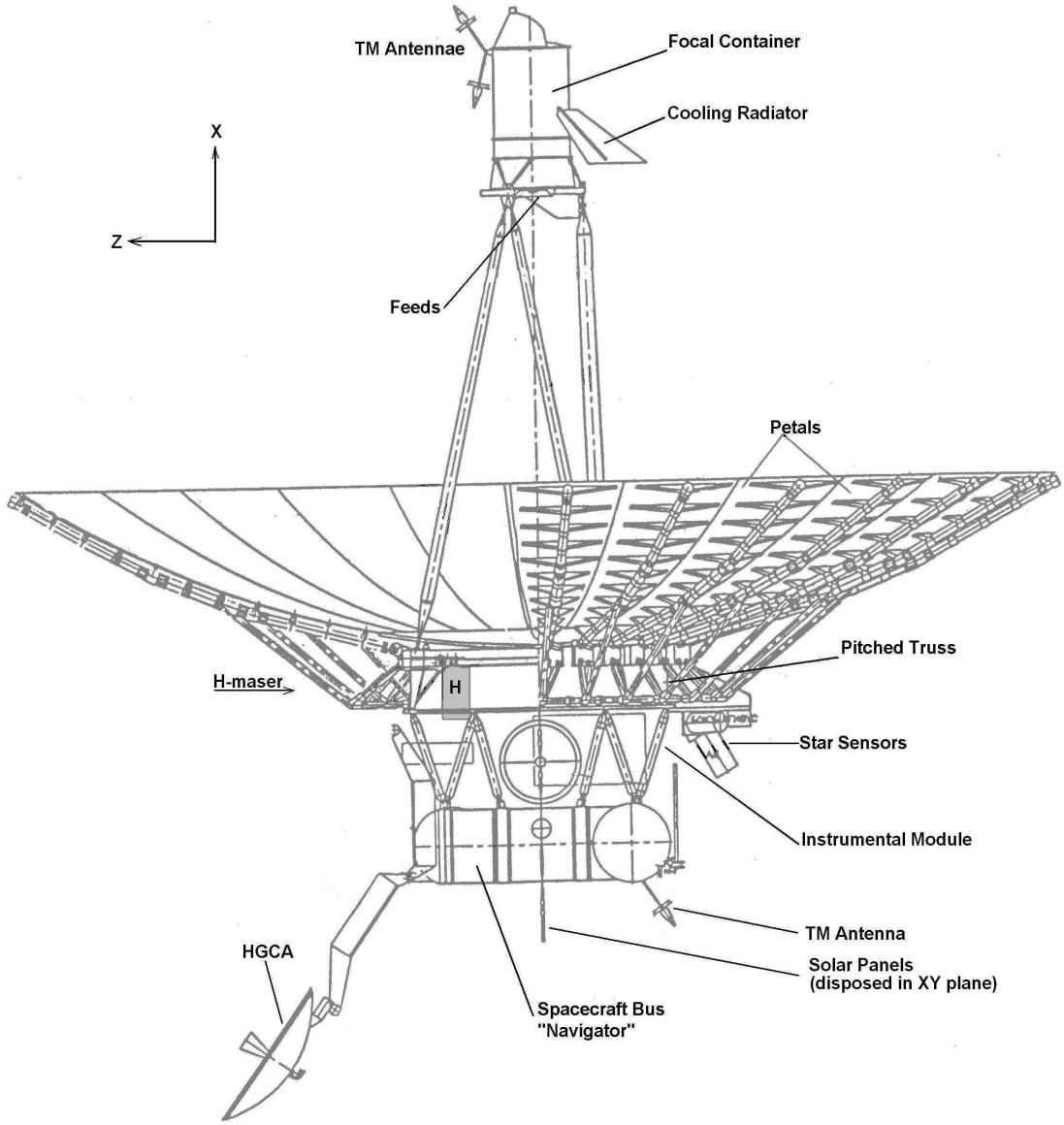

Figure 1: A sketch view of the RadioAstron satellite. The Space Radio Telescope (SRT) is serviced by the Navigator spacecraft bus. The solar panels lie in the Y-direction, i.e., perpendicular to the sketch plane. Component H is the high-precision Hydrogen frequency standard (H-maser).

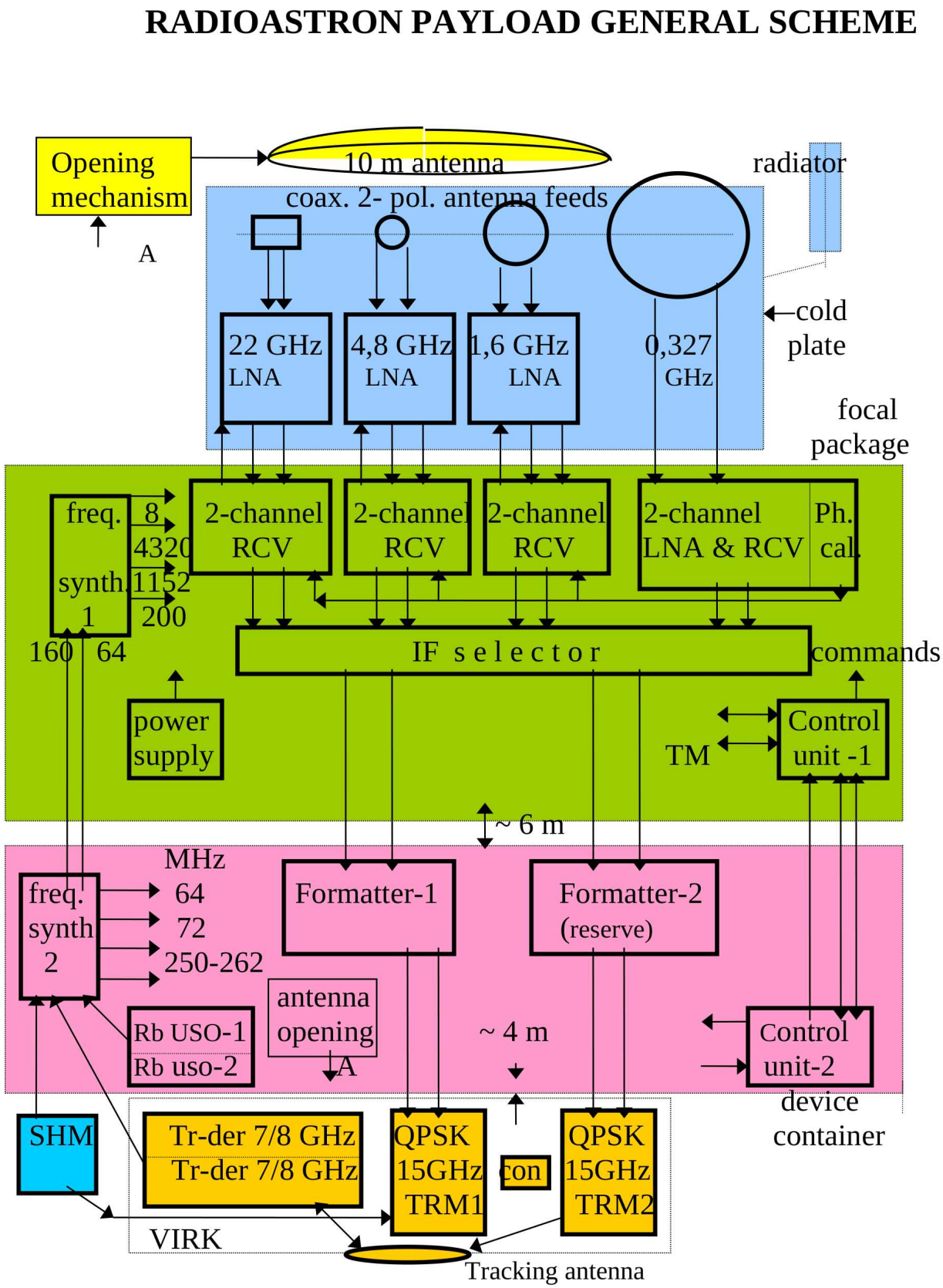

Figure 2: The general diagram of the on-board scientific complex. For an explanation of the abbreviations in use see Appendix B.

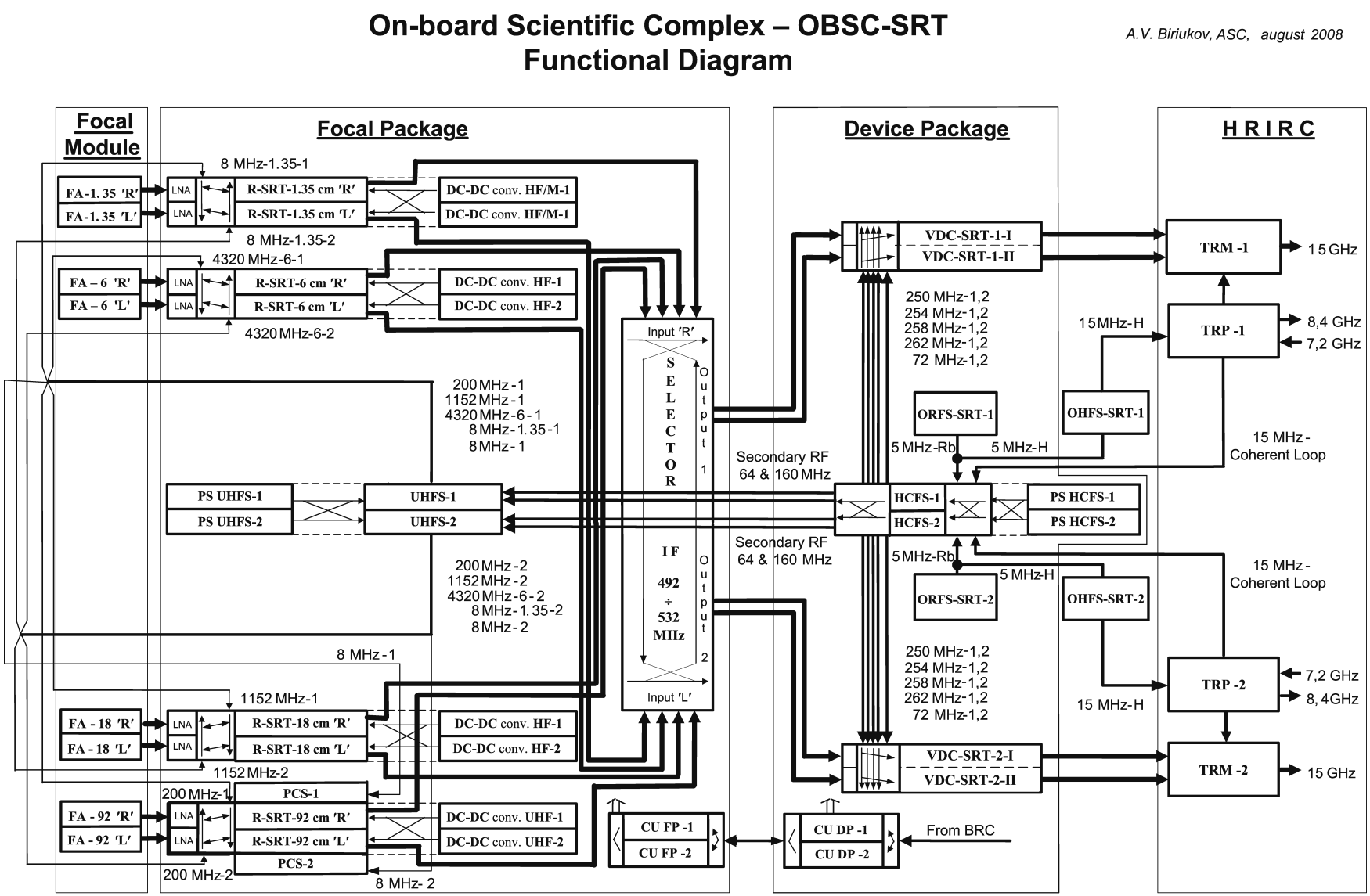

Figure 3: The detailed functional diagram of the on-board scientific complex. For an explanation of the abbreviations see Appendix B.

2.1.1 The Onboard Command and Measuring System (OCMS)

The Onboard Command and Measuring System (OCMS) also includes the Telemetry System (TMS). The TMS is a software-hardware package that is used for the acquisition, conversion and storage of telemetric information. TMS parameters are sequentially scanned by the telemetry system in accordance with TMS frame descriptions stored in the TMS-computer. There are three different TMS streams with different TMS programs, which may be generated separately or simultaneously. The first TMS stream may be sent to the OCMS for direct transmission to the ground and simultaneous recording in the memory. The second stream is intended solely for recording in the on-board memory. The third (digital) stream may be send to the TMS for direct transmission to the ground and simultaneous recording in the memory. During the mission, the TMS computer can be partly reprogrammed.

Spacecraft radio support is provided at C-band and includes:

- three command receivers,
- three receiver-transponders to receive commands and retransmit a signal to the Earth for trajectory measurements,

The spacecraft radio system can operate in the following main modes using omni-directional antennas:

- reception of commands from the ground,
- measurements of range and range rates,
- transmission of telemetry information in a direct transmission mode (in real-time) or in a memory playback mode at a rate up to 32 kbps.

2.1.2 The Spacecraft Onboard Control System (OCS)

The spacecraft Onboard Control System (OCS) has the following major functions:

- setup of base three-axis orientation from an arbitrary initial position;
- orientation of the axes of the SC in a given direction and stabilization relative to this direction;
- controlling operation of orbital correction engines;
- pointing the HDRC high-gain antenna to the Earth tracking stations.

The following components are incorporated into the OCS to carry out the aforementioned functions:

- sensor elements;
- on-board computer;
- interface instruments;
- movement execution devices.

The three star sensors are combined in an astro-system mounted on the pitched truss of the SRT. The directions of the optical axes of these star sensors will be described in section 2.4.1. Each star sensor

has an objective lens with a diameter of 25 mm and a focal distance of 52 mm, and a field of view of 12°. The OCS can be used for stars down to 6^m.

The on-board computer contains a star catalog and the OCS can identify the SC orientation without any preliminary information. For precise pointing and stabilization, two star sensors are used simultaneously. The OCS provides an accuracy of $\pm 10''$ as the maximum random error. Systematic errors connected with thermal deformations are determined by bore-sighting measurements (see section 2.5).

Inertial devices and a jet system are used to control the orientation of the spacecraft. A total of eight reaction wheels are used for maintaining the "fine" mode of the SC orientation and for re-pointing. The hydrazine thruster jet system is intended as first-order system for the SC orientation, the unloading the reaction wheels, and for orbit corrections. There are 12 thrusters in total: 4 for coarse traction, and 8 for fine traction. The control system can provide as many as 15 automatic re-pointing operations during a scientific observation session. The settling time after each re-pointing is about three minutes. The slew rate is 0.1 deg/s. When the angular distance between successive observing sources exceeds 10 degrees, a new calibration of star sensors and attitude control devices is needed to provide high accuracy of tracking; this calibration takes about 30 minutes.

2.2 Scientific payload

The science payload consists of a space radio telescope, feed arms, a focal container, an instrumentation module, a high data rate communication system with a high-gain antenna, and two separate on-board Hydrogen maser frequency standards.

2.2.1 Space Radio Telescope (antenna)

The Space Radio Telescope (SRT) with a diameter of 10 m and a focal length of 4.22 m operates in four frequency ranges: 0.316–0.332 GHz (P-band), 1.636–1.692 GHz (L-band), 4.804–4.860 GHz (C-band), and 18.392–25.112 GHz (K band). In order to achieve a high surface accuracy, the SRT consists of a solid central mirror of 3-m in diameter surrounded by 27 solid petals ($34 \times 115 \times 372$ cm) made of carbon-fiber. The maximum deviation for the surface from a paraboloid must not exceed ± 2 mm. In the initial folded configuration, the whole construction occupied a cylindrical volume of 3.6×7.6 m. The process of unfolding the SRT in orbit was achieved by a single motor, which causes the synchronous rotation of each petal over its own specially inclined axis and a cylindrical hinge. Finally, the whole construction is fixed by pins at each petal fastening them altogether. Each petal is also fixed in position with a cross brace. The petal framework is made of carbon-fiber tubes, which is covered by a surface with a three-layer composition including carbon-fiber trimmings combined with aluminum honeycomb. The surface of a petal could be adjusted before launch by means of 45 special screws over a range of ± 7 mm. The solid central mirror of the dish is fixed to a pitched truss by nine connecting bolts that eliminate the influence of thermal deformation of the pitched truss. The pitched truss itself is a cylindrical ribbed construction made of aluminum alloy. The truss serves as basic structural element for the SRT; it carries all petals, the central mirror, six supporting legs of the focal container, and all unfolding devices. In addition, the star sensors are placed at the pitched truss to reduce the effects of thermal deformations in operating the OCS.

The required high reflectivity of the SRT surface (98%) is provided by an aluminum coating of $100\mu m$ thick. To reduce thermal deformations of the SRT, the tubes of the petal framework were designed to be thermo-stabilized by special heating elements keeping the temperature within $\pm 50°$ C, however, IOC testing revealed this temperature stabilization system had failed, and so the petal framework is at natural thermal equilibrium with a temperature gradient of about 50° C across the dish. However, the pitched truss itself stayed under the control of thermo-stabilization. At the rear, the petals are shielded

by multi-layer thermal isolation. According to the functional constraints (see section 2.2.7), the Sun must not illuminate the SRT dish surface. Such conditions provide stability for the temperature field. Measurements conducted by the bore-sighting on strong radio sources at the highest frequency range (1.35 cm) confirmed the stability of in-beam pattern and in-beam offsets.

2.2.2 The Feed System

The feed system is located at the prime focus of the paraboloid and is attached to the bottom of the focal container. Fine-tuning of the position of the whole system was possible over a range of ± 7 mm during its assembly before launch. The feeds for 92, 18 and 6.2 cm wavelengths are ring resonators, while the 1.19–1.63 cm feed is a conical horn. The concentric design provides the possibility of observing at two different frequencies, or, alternatively, at two circular polarizations simultaneously.

2.2.3 The Receivers

Radio astronomical receivers at each frequency range have two independent channels to accept signals with right-hand and left-hand circular polarization (RCP and LCP) from the feed system. All receivers are located in the focal container. The low noise amplifiers (LNA) utilize high electron mobility transistors (HEMTs). The L-, C-, and K-band LNAs are located on a "cold plate" with a passive cooling system, which is expected to maintain a temperature of about 130 ± 20 K. The LNA for the P-band receiver operates at a physical temperature of 303 ± 3 K. The first stage of each receiver is kept at a constant temperature of 43 ± 1.5 °C by a thermo stabilization device, while the temperature in the focal container itself is kept within a 5–35 °C range.

The LNAs are connected to the receiver units using semi-rigid coaxial cables. The P-, L-, and C-band receivers are designed with the single frequency conversion to 512 MHz (L- and C-band), and to the 524 MHz (P-band) central IF frequency. The conversion for K-band Multi Frequency Synthesis is more complicated and will be described later. The IF output signal of each receiver can be attenuated by 0–31 dB with steps of 1 dB, in order to adjust the input level for the Formatter. The operating bandwidth of the IF output signal is 16, 64, 64, and 320 MHz, respectively for the P-, L-, C-, and K-band receivers.

The microwave selector provides channeling of two IF signals (two polarizations or two frequency bands with opposite polarizations) by cables, running along the support legs of the focal container, to the formatter located in the instrumentation module. In addition to the IF output, each receiver provides power levels detected with a 1 sec time constant in the bandwidths mentioned above. These power levels are digitized with a 12-bit ADC, and stored in on-board memory to be used for calibration and bore-sighting.

2.2.4 The Formatter

The Formatter receives two IF signals and converts them to a video band, where they are digitized with a 10-bit ADC at the 64 MHz sampling rate. Subsequent digital filtering is used to form the upper and lower side bands of 4 or 16 MHz wide. The Formatter operates with one-bit sampling at Nyquist frequency. Finally, the Formatter forms two binary data streams corresponding to two polarizations or two frequency channels (a parity bit being added to every byte). These data streams are transmitted to the ground tracking station using a QPSK modulation at a rate of 18×2 or 72×2 Mbit/s. Each stream consists of a sequence of data frames each containing 20,000 bytes: 30 bytes of data header and 19,970 bytes of science data. The header replaces the science data.

The header contains a synchro-code (7 bytes) and a frame counter (2 bytes) in the range of 1–400, which covers the recording time of 1 or 4 seconds as required by the above data rate. The header contains information about the current configuration of the science complex. The first 10 bytes of the header are used for the spacecraft telemetry system, which uses these bytes to form standard telemetry frames by inputting data into successive headers. At the tracking station these TM-bytes will be identified, selected, and transferred to the Flight Control Center for near–real-time analysis.

The frequency plan of the different configurations of the Formatter will be presented in section 4.1.

2.2.5 High-Data-Rate Communication radio links (HDRC)

The high-data-rate communication radio link system provides:

- Transmission of science data to the ground tracking station. The central frequency is 15 GHz, the modulation mode is QPSK, the maximum data rate is 2×72 Mbps, and the transmitted power can be selected to be either 40 W (for near apogee) or 4 W (for near perigee).
- Reception of the reference tone signal from the TS with a nominal frequency of 7.2075 GHz, and transmission a response at 8.4 GHz (2 W), thus providing an up-down link loop.
- Coherent conversion of the received tone to a 15 MHz reference frequency to be used in the operational mode with external synchronization (alternative to synchronization of the on-board Hydrogen maser).

To provide the required power for communication at the longest distances (near apogee), the HDRC system utilizes a 1.5-m diameter high-gain communication antenna (HGCA) made of carbon-fiber. The bi-axial drive of the HGCA allows pointing toward the selected ground tracking station (for more details see Section 2.4.1).

2.2.6 The System of Frequency Synthesis (SFS)

The system of frequency synthesis includes frequency standards and frequency synthesizers. In the external SFS mode, a reference frequency of 15 MHz is formed from the coherent tone signal, received from the ground TS at a frequency of 7.2 GHz. In the internal SFS mode, the H-maser frequency standard provides a reference frequency of 5 MHz for the science system. The H-maser can also provide a 15 MHz reference signal for the HDRC operation, or the HDRC may utilize the 15 MHz reference signal obtained from up-down link loop, while all frequency synthesizers are being fed with the H-maser output (5 MHz, or 15 MHz). In other words, operations without the up-down link loop are possible, and combined modes using both the up-link and internal H-maser synchronizations are also possible. An additional on-board Rubidium frequency standard (RFS) can be used for equipment testing and antenna measurements.

All local oscillator frequencies are generated by the high-frequency synthesizer (HFS) located in the focal container, while secondary LO-frequencies used by the Formatter are generated by the low-frequency synthesizer (LFS) installed in the instrumentation module. The LFS also provides a sampling frequency. All SFS devices, including the H-maser standard, have a secondary unit for redundancy. The on-board Hydrogen maser (VCH-1010) weighs 60 kg and has a size of 460x729 mm (diameter and height). It has a relative frequency uncertainty of 3×10^{-13} for 1 s, 3×10^{-14} for 10 s, 7×10^{-15} for 100 s, and 3×10^{-15} for 1000 s. A separate frequency synthesizer, as part of the receiver, is used for multi-frequency operation at 18.392–25.112 GHz.

The frequency plan for all observable frequencies is described in Section 4.1.

2.2.7 The Control System (CS)

The Control System (CS) receives commands from the TMS or the TPS spacecraft systems and distributes these commands among the different devices of the science payload. The CS consists of two units: a Control Unit located in the focal container (CUFC) and a Control Unit in the Instrumentation Module (CUIM), which are responsible for the science equipment located in the respective container.

There are two types of commands: operational commands and digital commands. An operational command represents a pulse issued by the TMS/TPS to the CS using the selected electric bus line. In response to this pulse, the CS switches voltage to the necessary relay in order to turn on the power for a receiver, for example. Digital commands are issued by the TMS/TPS to the CS or directly to the selected device, where they will be decoded and result in the required action.

2.3 RadioAstron orbit

The RadioAstron satellite is flying in a moon-perturbed orbit, where the orbital elements have been chosen to maximize their evolution by weak gravitational perturbations from the Moon and the Sun.

2.3.1 Initial orbit elements and their evolution

After an orbit correction was successfully performed on March 1, 2012, the orbit is expected to have ballistic lifetime greater than 9 years and the orbiting SC will spend no more than 2 hours in the Earth's shadow in each orbit. The initial orbital elements for the epoch April 14, 2012, are the following:

- semimajor axis = 174714.234 km;
- eccentricity $e = 0.692$;
- ascending node-perigee angle $\omega = 303°$;
- inclination of the orbit $i = 79.69°$;
- longitude of ascending node $\Omega = 300.55°$;
- time of perigee transit 07:12:37.00 UTC on April 14, 2012.

The initial orbital period is about 8.5 days and the state vector for 07:12:37.00 UTC on April 14, 2012 is expressed as:

$$X = -113725.826\,\mathrm{km}, Y = 206789.091\,\mathrm{km}, Z = 39402.750\,\mathrm{km}\,;$$

$$V_x = 0.117640\,\mathrm{km/s}, V_y = -0.513834\,\mathrm{km/s}, V_z = -0.878956\,\mathrm{km/s}\,.$$

The evolution of this orbit is illustrated in Figures 4, 5, 6, 7, 8. The perigee will vary from 7,065 km to 81,500 km, the apogee will vary from 280,000 to 353,000 km, and the eccentricity of the orbit changes from 0.59 to 0.96. The characteristic period of these variations is about three years. Figure 8 shows the equatorial coordinates for the evolution of the direction of orbital normal. The evolutionary time scale is indicated by numbers of years, starting with zero for April 14, 2012. The vector circumscribes an ellipse of 150° by 45° in about 4–5 years. This evolution provides the possibility of observing many radio sources close to the orbital plane with moderate angular resolution.

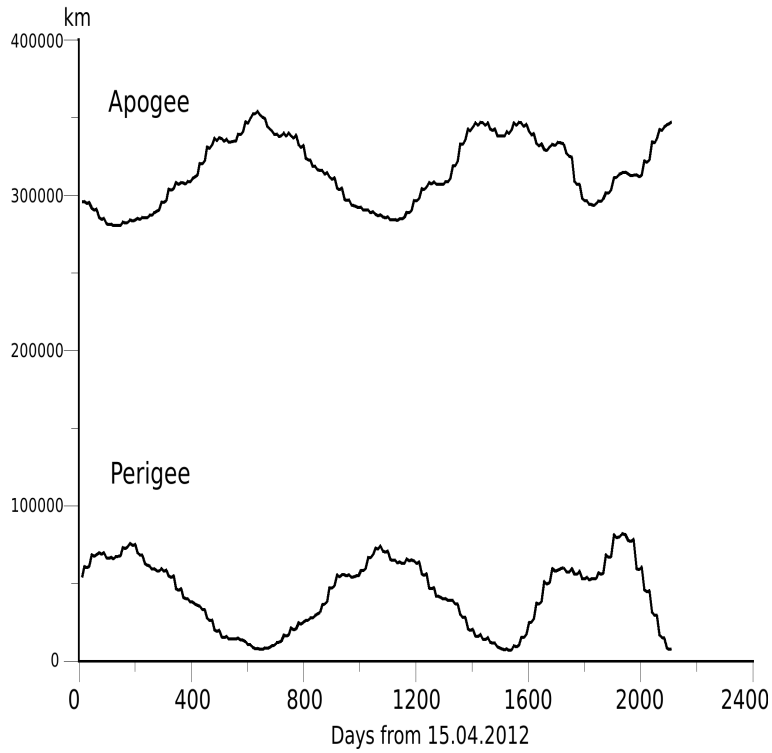

Figure 4: The variations of the perigee and the apogee heights over the five years from April 2012.

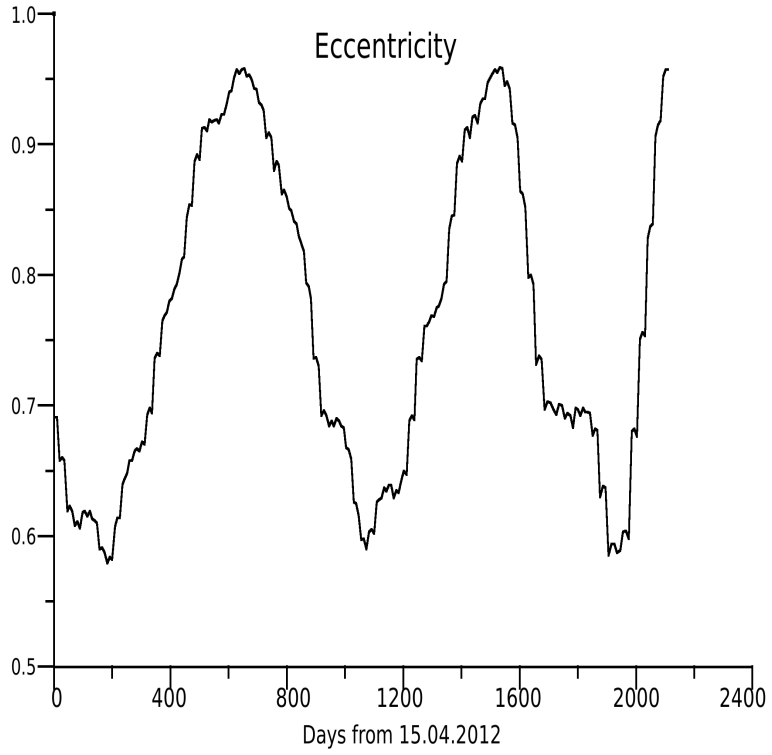

Figure 5: The variations of the orbit eccentricity over the five years from April 2012.

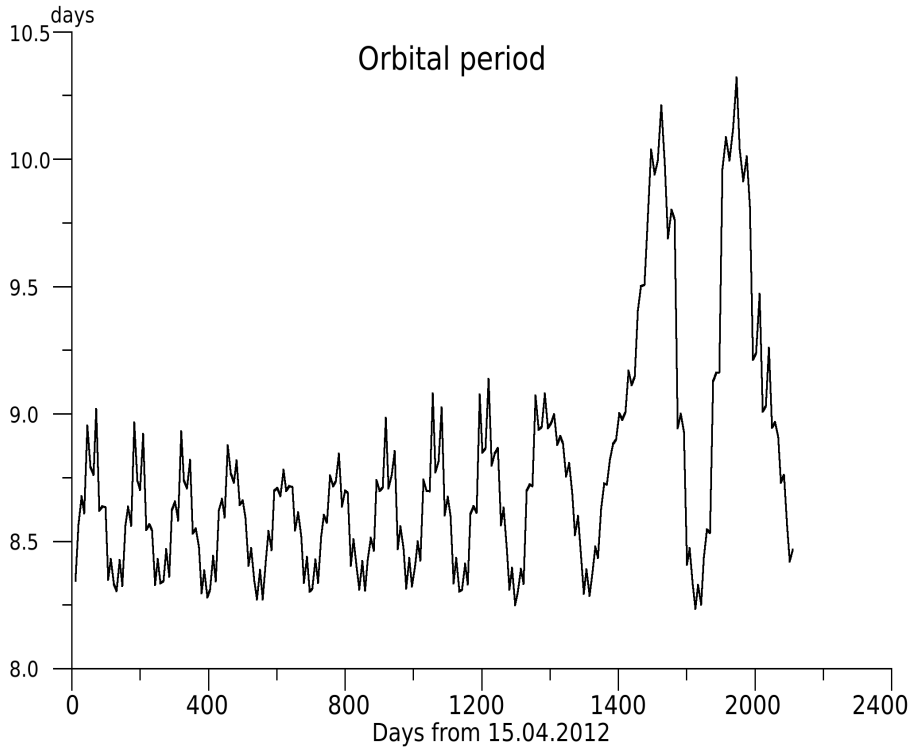

Figure 6: The variation of the orbital period over the five years from April 2012.

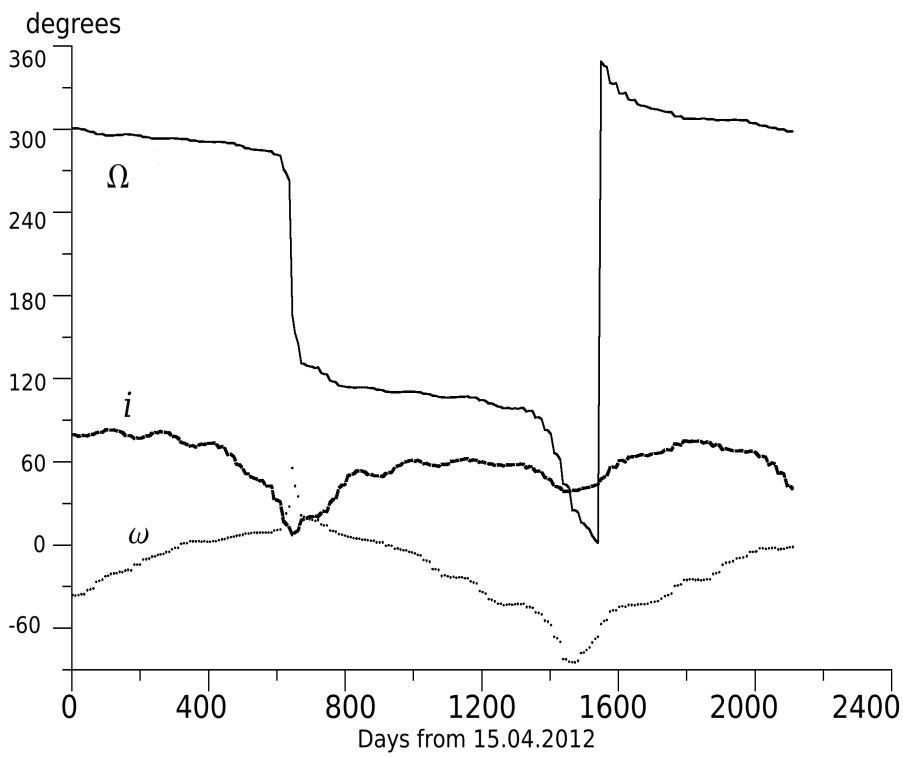

Figure 7: The variation of orbital elements (i, ω, Ω) over the five years from 2012.

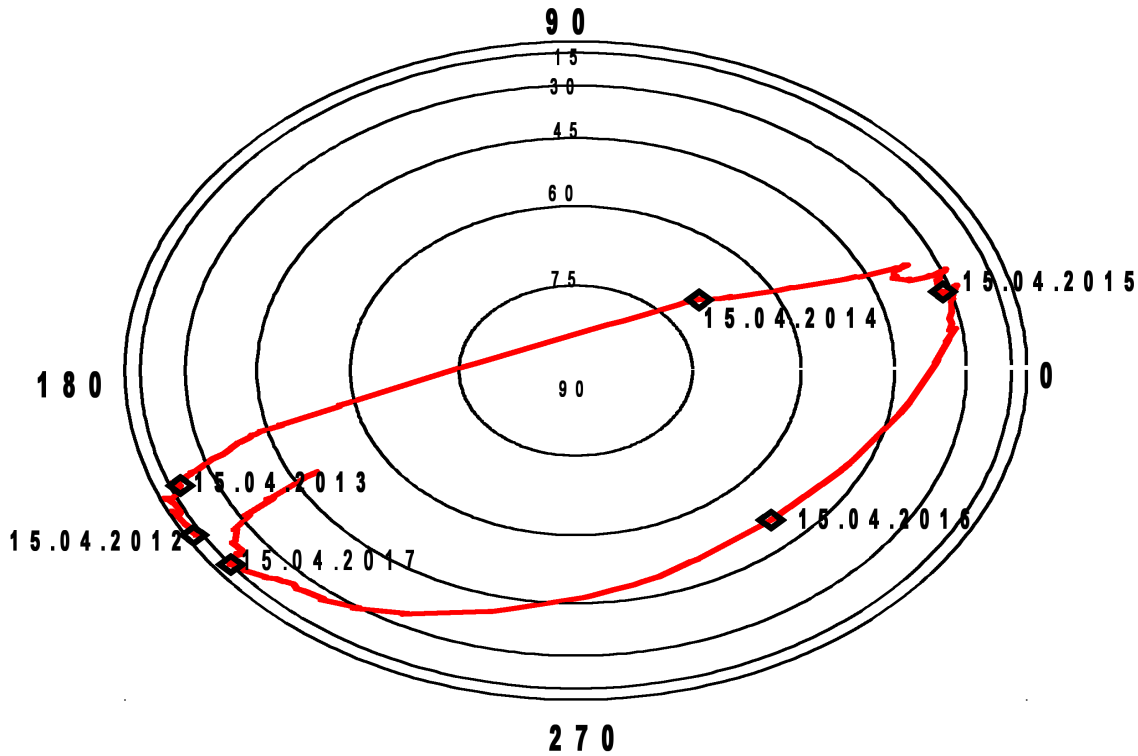

Figure 8: The evolution of the direction of orbital normal over the five years from 2012 (in equatorial coordinates).

2.3.2 Orbit Measurement (OM), prediction, and reconstruction

From a ballistic point of view the SRT is a difficult object because the solar radiation pressure affects the elements of the spacecraft construction differently. As a result, a force-moment appears around the spacecraft center of mass. The reaction-wheel system (RWS) will be used to maintain the spacecraft orientation. Long-term effects of these force-moments lead to a permanent increase of angular momentum that requires unloading of the spinning reaction wheels by switching the gas engines on. Such operations result in perturbations of the motion of the SC center of mass. Estimates show that the velocity changes caused by such perturbations can reach values of 1–5 mm/s. There are three sources of OM data:

- orbit measurements made at C-band (command and telemetry radio link),
- orbit measurements made at X-band during science data transmission using the up-down link loop of the HDRC (radial velocity only),
- specific measurements using laser ranging stations.

The first kind of OM includes range and range-rate measurements made by the Command & Telemetry Station facilities located at Bear Lake (near Moscow) and at Ussuriisk. The range-rate ($\dot{\mathrm{R}}$) is measured by a Doppler method using a carrier frequency in the C-band in coherent two-way mode using a 10 s integration interval. Systematic and RMS equipment errors of the $\dot{\mathrm{R}}$ measurements are $\sigma(\dot{R}) = 0.2\,\mathrm{mm/s}$. The range R is measured using a phase measurement with sub-carriers at 0.03, 0.3 and 1.2 MHz. Systematic and random RMS errors of the range measurements are $\sigma(R) = 20\,\mathrm{m}$. The duration of trajectory measurements in the C-band will generally not exceed 8–10 minutes.

Orbit measurements using the HDRC radio channel only give the radial components of the SC velocity, but such measurements can be done continuously during observing sessions using any tracking station that receives the scientific data. The RMS errors of these measurements are $\sigma(\dot{R}) = 0.1$ mm/s. Orbit measurements by laser ranging techniques can only be done after reorientation of the SC but would provide an accuracy of $\sigma(R) = 10$ cm.

Ballistic navigation information of the RadioAstron SC will be made available to other parties (agencies) in order to perform orbit reconstruction and other control activities and will include:

- the state vector of the spacecraft at the time of definition of the orbit with respect to the trajectory measurements,
- the radial velocity measured by ground tracking stations,
- information about the attitude of the space radio telescope (SRT) antenna and the solar battery panels,
- information about SC maneuvers,
- the ephemeris of the spacecraft.

The accuracy of the orbit prediction depends on the kind of trajectory measurements that were used for the orbit reconstruction. The typical accuracy in position and velocity is (maximum difference with the true orbit):

- for planning the orbit (for spacecraft operations, 30 days in advance): 3000 m and 0.50 m/s,
- for predicting the orbit (for tracking stations, 3–7 days in advance): 1500 m and 0.2 m/s,
- for reconstructing the orbit (for scientific observation and correlation): 500 m and 0.02 m/s. A reconstructed orbit is available 2–3 weeks after the science observations.

2.4 Operational constraints

A number of physical and operational constraints affect the pointing of the on-board radio astronomy antenna SRT. A reference frame with a right-handed rectangular coordinate system would have the X-axis directed along the electrical axis of the SRT (see Figure 1), the Y-axis falling parallel to the rotation axis of solar panels, and the origin O located at the mass center of the spacecraft.

A general condition for the SC operation is that the SC can only be illuminated by the Sun from the +Z and −X directions. In this manner, the −Z hemisphere (the right-hand side of the SC in the figure) will mainly be in shadow.

2.4.1 Constraints connected with SC service systems

1. **Thermal Control System (TCS):** The angle between the +X-axis and the direction to the Sun must be in the range of 90–165° at half-plane XOZ (+Z) . In Fig. 1 the Sun will shine from the left and underneath the antenna surface. The deflection of the vector to the Sun from the half-plane XOZ must not exceed ±10°.
2. **Solar battery panels:** The angle between the normal to the solar panels plane and the direction to the Sun must not exceed 10°. Solar panels can be rotated around the Y-axis only.

3. **Star sensors:** Three star sensors are mounted on a single plate fixed at the pitched truss carrying the SRT dish (see section 2.2.1). Only two star sensors need to be used to establish a three-axial SC orientation.

   The optical axes of two star sensors (AX1 and AX2) are directed in the following manner: a) the axes AX1 and AX2 are placed in a half-plane inclined by 15° to the half-plane YOZ with −Z-axis in the direction of the −X-axis, b) the angle between the AX1 and the −OY axes is 45°, and c) the same angle of 45° exists between the AX2 and +OY axes. The AX0-axis of the third sensor is located in the XOZ-plane with an inclination from the −X-axis by 30° in the direction of the −Z-axis.

   According to the Lavochkin Association, the measurement of star sensors coordinates in the SRT system before launching the RadioAstron spacecraft on July 2012 gave values for directional cosines of star sensors axes as follows:

	AX1	−0.86640913, −0.00055799, −0.49933447
	AX2	−0.18425467, −0.70842875, −0.68130677
	AX0	−0.18282000, 0.70791153, −0.68223024

   There are certain angular constraints on the positions of the Sun, Moon, and Earth in context of mutual orientation of the star sensors. Angles of each star sensor from any combination of two star sensors must to meet constraints on the positions of these celestial bodies as follows. The offset angles must be > 40° from the Sun center, and > 27° from nearest edges for both the Moon and Earth.

4. **High-gain communication antenna (HGCA):** The HGCA provides communication with the tracking station for data transfer and frequency synchronization. Science observations with the RadioAstron SRT are possible only when such communication is in operation. The HGCA is mounted at the bottom edge of the service bus NAVIGATOR (see Figure 1). The axis X_A of the HGCA lies in the XOZ plane of SRT system and is oriented by 17.5° from the −X-axis in the direction toward the Z-axis of the SRT system.

   The HGCA has a bi-axial drive using the Y_A and Z_A rotation axes. The Y_A rotation axis is parallel to the main Y-axis, and the Z_A rotation axis forms a right-handed coordinate system. In this $X_A - Y_A - Z_A$ reference frame, the HGCA 1.5-m dish can be directed to any point of the hemisphere around the X_A-axis according to the following constraints. The HGCA 1.5-m dish can be rotated around the Y_A-axis from −73° to +90°, and can be rotated around the Z_A-axis from −90° to +90°. To be complete, there are two small forbidden areas in this hemisphere, namely, the spherical segments near the Z-axis with cone angles of 12.5° and 4.5° for the +Z and −Z poles, respectively. These exclusion areas are connected with the constraints for the rotation of the antenna around the Y_A-axis.

   According to the Lavochkin Association the electric axis of the HGCA is displaced by 14.76° relative to axis X_A of the gain in the XOZ plane of SRT system to the Z-axis of it.

   Finally, the axes of of the HGCA have next the directional cosines in the SRT coordinate system:

   X axis has coordinates −0.95585102, −0.00818895, +0.29373758 ;
   Y axis has coordinates −0.00960202, +0.99994823, −0.00336890 ;
   Z axis has coordinates −0.29369479, −0.00604064, −0.95588015 .

It has been found that HGCA drive motors overheat in long operations. The degree of this overheating depends significantly both on the Sun angle and on the HGCA current position. In general, the longest observing session possible is about 4 hours, with a 3 hours gap then required before the next observations. Other ways to conduct long observations are to use a cycle consisting of one hour's work and a two hour break, or 30 minutes' work and a 90 minute break.

2.4.2 Constraints connected with the science payload

1. **The LNA and feeds passive cooling system:** The angle between the −Z-axis of the SRT system and the Sun must be larger than 90°. Moreover, the Sun must not illuminate the surface of the cooling radiator, which represents a frustum with the X-axis as a main axis and an opening angle of 60°. The conical surface is outlined by the di-hedral angle of 60° (±30°) relative to the −Z-axis. The angle between the −Z-axis and the direction to the Earth center must be larger than 30° for geocentric distances of the SC less than 20,000 km.

2. **The thermal conditions for the SRT dish surface:** The surface of the SRT dish must not be exposed to the sunlight, i.e., the angle between the +X-axis and the Sun must be larger than 90°. In fact, conditions 1 and 2 are less restrictive than condition 1 in Section 2.4.1.

3. **The radio astronomical receivers:** The angle between the +X-axis of the SRT system and the direction to the Moon center must be larger than 5°. The angle between the +X axis and the direction to nearest edge of the Earth's limb must be strictly larger than 5°.

2.5 Pointing offsets and gain measurements

The Spacecraft Onboard Control System provides two possibilities for pointing and gain measurements:

1. Drift rotations of the spacecraft round the axis Y, and Z with constant angular velocities (18″/s and 36″/s) in two perpendicular directions may be initiated in a such a manner that the trajectories of these two scans produce a rectangular net on the sky with the observed radio source in the center. The full span of each drift scan is 1°, 5°, 12.5°, and 20° at 18–25, 4.85, 1.65 and 0.327 GHz, respectively.

2. Successive pointing of the antenna using a series of points close to the radio source at equidistant angles on a rectangular grid or the cross-like structure. The integration time for each point may be 1–10 minutes. This is the equivalent of a five-point procedure.

Bore-sightings were conducted during the In-Orbit Checkout (IOC) period to determine the SRT beam structure and the initial pointing offsets. It was found that in P, L, and C frequency ranges, beam half-width corresponds to the specifications (370′, 72′ and 25′). At K-band the beam shape was found at 22228 MHz to be elliptical with half-widths of 360" by 780" (compared to the expected value of 340"). Such a deformation and its accompanying loss of antenna efficiency may be caused by thermal deformations or other reasons. At K-band, beam offsets of $-2.5' \pm 1.2'$, and $0' \pm 1.2'$ were measured around the Z and Y axis correspondingly. Antenna gain calibrations are carried out weekly to control gain stability, beam pattern and offsets. It was found that, despite the failure of thermal stabilization, beam pattern and offsets were not changing with time within the accuracy of measurements.

For gain measurements (scanning or pointing), the power levels from a given receiver output (using the total bandwidth before the IF-system) is being recorded into the on-board telemetry memory, together with the required data from the Onboard Control System. This combined data are transmitted directly to a ground telemetry stations during a control session or afterwards. Pointing offsets and gain corrections are determined using off-line data processing.

2.6 Calibration

2.6.1 Noise calibration

Each frequency receiver has a noise calibration signal generator that injects a noise signal into the LNAs. There are two levels of Noise-Cal power: a high-level Noise-Cal that equals about half the system temperature T_{sys}, and a low-level Noise-Cal that constitutes a few percent of T_{sys}. The ON/OFF switch of the Noise-Cal generators can be operated by the commands: a sequence of calibration events may be stored in the spacecraft Time-Program System (TPS) for future execution. Such events are being scheduled to be conducted just before and after the every observing set. The results are recorded both in total band of a given receiver and in each specific IF subband.

2.6.2 Pulse calibration

A pulsed calibration signal can be injected into the LNAs at P-, L-, and C-bands; for the K-band it is injected at the IF frequency. The power level of the injected pulses is equivalent to 1–3% of the receiver noise. The pulse repetition period is 1μs and the spectrum of the signal with pulse injection will show narrow harmonics separated by 1 MHz. These calibration tones will be detected and analyzed during data correlation. The pulse calibration system is switched off for maser and pulsar observations.

3 RadioAstron Ground Segment and Operations

The ground segment of RadioAstron consists of Control Stations (CS) for operating the satellite, Laser Ranging Stations for tracking the satellite position, Tracking Stations (TS) for receiving the satellite data, Ground Radio Telescopes (GRT) co-observing with RadioAstron, Ballistic Center for orbit prediction and reconstruction, Correlator Facilities for data processing, and dedicated communication lines for fast data e-transfer.

3.1 Tracking stations

Currently, two tracking stations are being routinely used by the RadioAstron Mission: one is based on the 22-m radio telescope of the Pushchino Radio Astronomical Observatory (PRAO), and the other on the 140-ft telescope in the National Radio Astronomy Observatory, Green Bank, WV, USA (GBES). The hardware configuration of the TS and signal distribution and transformation are shown in the diagram presented at the RadioAstron web site[3].

The TS performs the following functions:

- Tracking the spacecraft in its motion along the sky during the communication session.
- Receiving binary stream science data at a 15 GHz central frequency with QPSK modulation at a maximum rate of 144 Mbps, decoding the data, and recording 128 Mbps with the RDR or Mk5C recording system.
- Selecting telemetry information (TM) from the frame-headers of the science data stream, recording the TM information, and distributing this TM-data among the customers in a near real-time fashion.

[3] `http://www.asc.rssi.ru/radioastron/documents/memo/2006/memo7/ts.htm`

- Extracting the current 15 GHz carrier in the science data stream, and measuring the residual phase relative to the H-maser frequency standard.
- Transmitting to the SC of the reference tone signal synchronized in phase with the H-maser frequency standard at 7.2 GHz.
- Receiving the reference signal from the SC that is coherently transformed from 7.2 to 8.4 GHz.
- Measuring the full and residual phase, and recording the results.

3.2 Ground radio telescopes

The 10-m space radio telescope (SRT) has a relatively small effective area. Consequently, the use of the largest ground radio telescopes provides the highest possible sensitivity and provide more efficient observations. A radio telescope with a diameter larger than 60-m in conjunction with the SRT will have a baseline sensitivity similar to two 25-m dishes. Many ground radio telescopes have successfully participated in experiments with RadioAstron including EVN and LBA stations, Evpatoria, Usuda, Tidbinbilla, GBT, and Arecibo.

Observing time at ground radio observatories can be obtained on the basis of regular proposals or special telescope time commitment. More details on obtaining scientific access are given in Section 3.7 and the Announcements of Opportunity for the RA Mission.

3.3 Data recording

The RadioAstron Data Recorders (RDR) are used at the TS in Pushchino, Green Bank, as well as Kalyazin and Evpatoria GRTs. The RDR was developed and manufactured at the ASC. It utilizes a rack of four disks under the control of a PC. The main processor is a P4-3.06 GHz, the data input controller is a PCI-7300A, and the RAID-0 output controller is a Fast Track 100TX. The recording rate is 128 Mbps, the number of digital input channels is 8 or 16. The RDR operates under external synchronization using 1 Hz and 32 MHz. The RDR takes data from the Data Acquisition System (DAS) of the ground radio telescopes, and from the science data decoder at the TS.

Mk5A, Mk5B, and Mk5C data recording at ground radio telescopes is possible. See the next section for a discussion of data correlation. Mk5C recording is also possible at the GBES.

3.4 Data correlation

3.4.1 ASC correlator

Data correlation is performed by the ASC processing center of the recorded data flows (256 Mbps versus 256 or 128 Mbps), including the SRT.

ASC software FX-correlator is organized on a cluster processor of 1 Tflop/sec power and RAID-array storage device of 1 TB total capacity. Software realization of FX-mode correlator for multiple baseline interferometer can be shown by the following executable phases:

- Direct Fourier Transform (Direct FFT) of data from each single interferometer element, corrected for relative delay and fringe rotation (Doppler frequency compensation) at each station.
- Pair multiplication of the resulting Direct FFT.

- Reverse FFT of the resulting cross-spectrum (transition from frequency to delay interferometer response).

This sequence of processing steps, as compared to hardware correlators, gives rise to efficiency of data processing and allows provisions for multi-mode control without additional financial expenses. For pulsar observations, the ASC correlator provides gating and dedispersion. The ASC software correlator accepts data flow in practically any of the existing VLBI data formats. Data synchronization (with accuracy of fractions of microseconds) is accomplished by means of high precision analytical models of the satellite and Earth motion, supported by actual remote measurements of the satellite orbit from the Keldysh Institute of Applied Mathematics.

The ASC Cluster can receive data from up to 10 stations (including the SRT) at 2.56 Gbit/sec and so can correlates 45 independent interferometer baselines. In practice, this can take place without considerable reduction from the real time data rate.

3.4.2 DiFX correlator

The DiFX software correlator was upgraded by the Max-Planck-Institute for Radio Astronomy in Bonn and is capable of correlating RadioAstron data. See For more details Bruni et al. (2014)[4].

3.4.3 SFXC correlator

The EVN software correlator at JIVE (SFXC) has successfully detected fringes in a number of RadioAstron data sets at 1.6, 5 and 22 GHz, including spectral line fringes at the latter frequency. For additional details see EVN Newsletter 36[5] and Keimpema et al. (2015, Experimental Astronomy, 39, 259). RadioAstron-EVN/global-VLBI observations of AGN, masers, and pulsars can be correlated at JIVE by the SFXC correlator. SFXC can handle pulsar gating/binning.

3.5 Satellite operations and experiment scheduling

The Mission Operations Plan makes use of a long-term 2–3-month schedule (LTS) for a given trimester and short-term schedules (STS) for the current month. Both LTS and STS schedules are presented in a specific format agreed between ASC and the Lavochkin Association (LA). The observing schedules for observations within the LTS and STS will be created with the SCHED software by the RadioAstron Mission Scheduling Team (RMST) for all participating ground radio telescopes. It should be noted that in a case of an approved ToO proposal, the operations teams is able to schedule the SRT observations within 48 hours (if all observing constraints are satisfied).

To obtain observing time, scientists will need to submit proposals to Program Committees of RadioAstron and participating ground-based observatories or networks. It is also possible to secure access to ground radio telescopes on the basis of special agreements. In particular, radio telescopes in Russia and Ukraine are used on the basis of separate agreements.

Mission operations will be carried out by the ASC RMST, in close interaction with the General Operative Control Group (GOCG) of the Lavochkin Association. The RMST will create the Long-Term Schedules in the agreed format for every trimester. The GOCG at LA will evaluate possibility to conduct the schedule and will inform the ASC RMST on the constraints. Then ASC RMST will convert the schedule into the spacecraft operation commands.

[4] http://pos.sissa.it/archive/conferences/230/119/EVN%202014_119.pdf
[5] http://www3.mpifr-bonn.mpg.de/div/vlbi/newsletter/36/

3.6 Observational modes and procedures

While narrow-band ($B = 2 \times 4$ MHz) modes are possible, they have not been used. Even in spectral line observations, broad-band ($B = 2 \times 16$ MHz) modes have been utilized in the correspondence with the frequency setup given in section 4.1. In these modes both USB and LSB are recorded, and so one of the sub-bands may not be useful. The ASC software correlator can provide required spectral resolution through the zoom technique. In standard configurations both RCP and LCP polarization channels are being recorded. Due to concentric feed construction two-frequency observations in any frequency combination are also possible. Note, that in two-frequency mode channels with the opposite sense of polarization will be used. Because of the low speed of the SRT near apogee, it may be useful to observe the source sequentially at different frequencies. The switching time between frequency channels is negligible, but this mode requires all receivers being used to be powered ON (including thermostats), thus increasing power consumption.

Spacecraft control is conducted on a daily basis. A control session takes from 2 to 4 hours depending on the volume of transmitted commands. Additional sessions of orbit measurements by radio and by laser take about 30 minutes each. All these events are scheduled by the LA group well in advance. RWS torque wheel spin-down procedures are added at a later stage of scheduling, when the main science program will be composed. Therefore there might be several iterations of scheduling between the ASC and the LA. Every day about 10 hours may be available for science observations. The continuous observing time for a single target can be in the range from 1 to 20 hr, however, due to the unexpected additional constraints caused by the overheating of the drive motor of the HGCA, long continuous observations are impossible (see more details in section 2.4). Up to 15 re-pointings are allowed between the control sessions. The settling time after each re-pointing is about 3 minutes. The slew rate is 0.1 deg/s. When the angular distance between successive observing sources exceeds 10 degrees, a new calibration of star sensors and attitude control devices is required to provide high accuracy of tracking; this calibration takes about 30 minutes.

The observing procedure (use of fringe finders, switching noise and pulse calibrations etc.) must be defined by the PI or the responsible science team. There is a special observing procedure performing cycling in pointing between the source under investigation and one or two reference sources located on the sky within a few degrees. The slew rate in this procedure is $0.005°$/s, and the setting time is about a minute. The observing time (on-source) can be specified as a parameter, but it must be equal for every sources (main and reference) in a given cycle. The number of cycles is also a parameter. These cycles do not count against number of re-pointings. The procedure may be used for astrometry or fringe calibrators.

The following fringe finders are recommended on the basis of the RadioAstron AGN survey results.
L- & C-bands: 0119+115, 0234+285, 0235+164, 0657+172, 0716+714, 0748+126, 0814+425, 0851+202, 0954+658, 1005+066, 1044+719, 1226+023, 1253−055, 1642+690, 2200+420, 2230+114.
K-band: 0235+164, 0529+483, 0716+714, 0851+202, 1226+023.
It should be underlined that variability of AGN cores results in changing compactness characteristics of the suggested fringe finders. There is no guarantee that a given suggested fringe finder will be compact enough at an epoch of your experiment. The best is to schedule two scans on two of the suggested calibrators if a fringe finder is needed for the planned experiment.

3.7 Science access

The RadioAstron mission began with a *commissioning phase*, or In-Orbit-Checkout (IOC) period. The first part of the IOC included an *engineering commissioning* with a spacecraft bus checkout, the unfolding of the SRT, receiver checks and tests of the radio astronomy antenna in single-dish mode

(bore-sighting), and communication tests with the tracking stations (using the HDRC system). The spacecraft bus checkout was completed by the end of September 2011. Tests of the radio astronomy antenna in single-dish mode were finished in the middle of November 2011; they included as well all communication tests with the tracking stations in Pushchino. The second part of the IOC was a *scientific commissioning phase* that consisted of tests of the SRT science payload in VLBI mode using large ground radio telescopes. For this process the largest ground-based radio telescopes were required, including those located in Russia.

The second phase of the IOC, although designed for engineering checkouts, provided the first scientific results of the mission. This IOC phase smoothly transitioned into a *scientific verification phase* — the Early Science Program (ESP). The ESP lasted from February 2012 to June 2013. The ESP objectives were to achieve high-quality, high-profile scientific results and to provide a bridge between the initial "experimental" mode of operations, observing, and data processing, and the "routine" operations that started after completion of the ESP. Observing time with the RadioAstron was committed for ESP observations, and these were coordinated by several Working Groups (WGs) — on AGNs, masers, and pulsars. The WGs were organized by the mission from individuals and institutions that had contributed to the RadioAstron project development.

A yearly series of open AO's for KSP and later also for individual PI driven projects (Guest Observing Time) are being issued by the Mission, with AO-1, AO-2, and AO-3 observations starting in July 2013, July 2014 and July 2015 respectively.

4 Observations with RadioAstron

4.1 The Frequency setup

Four frequency ranges are available for astronomical observations: 92-cm (P-band), 18-cm (L-band), 6.2-cm (C-band), and 1.19–1.63-cm (K-band). In each band, except C-band, two output channels produce circular polarization (LCP and RCP) signals, which may be used simultaneously. In the very first IOC receiver tests it was found that C-band receiver didn't function correctly when both polarisation channels were used. Later on it became clear that only one polarization channel (LCP) operates properly. Different frequency bands may be used instead of two polarizations, and such modes must be used for C-band observations. In principle, any frequency combination is possible, except that the two frequency channels will have opposite polarizations with an exception of C+K which will have LCP+LCP.

The RadioAstron IF-to-VIDEO converter (the Formatter) can operate at two sampling rates, 16 or 64 MHz. Low-rate sampling provides simultaneous sideband recording (LSB+USB) with a 4 MHz width in both polarization (or in two frequency ranges) with one-bit sampling. In narrow-band (4 MHz) mode the Formatter will generate a binary data stream of 36 Mbps. High-rate provides recording in two polarizations (RCP+LCP) or in two frequency ranges with two 16-MHz bands (LSB+USB). The resulting data stream has a rate of 144 Mbps with a parity control bit for every byte. Note, that the LSB spectra will always be inverted.

The High-Frequency Synthesizer (HFS) provides fixed LO-1 frequencies at 200, 1152, and 4320 MHz for the P-, L- and C-bands respectively. The K-band has a different setting and is treated separately. The first LO moves the selected frequency range to an IF of about 490–540 MHz, and supplies the input signal for the Formatter. The Formatter uses four LO-2 frequencies of 500, 508, 516, and 524 MHz in order to permit some tuning of the desired sky frequency. Table 2 gives the correspondence between the LO-2 and the central sky frequency values, i.e., the frequency that separates the lower and upper sub-bands (LSB/USB). For K-band, only the main sky frequencies are indicated, and details are given

Table 2: The frequency set for the RadioAstron SRT

LO2-frequency (MHz)	Designation	P-band	L-band	C-band	K-band
500	S1		1652	4820	22220
508	C2		1660	4828	22228
516	C3	316	1668	4836	22236
524	S4		1676	4844	22244

Table 3: The observing modes for the RadioAstron SRT

N	Observing mode	Channel 1 - LCP		Channel 2 - RCP		BW (MHz)
1	**m92LRC3**	–	316–332	–	316–332	2×16
2	**m92L18RC3**	–	316–332	1652–1668	1668–1684	16+2×16
3	**m92R18LC3**	1652–1668	1668–1684	–	316–332	2×16+16
4	**m6L135LC2**	4812–4828	4828–4844	22212–22228	22228–22244	2×(16+16)
7	**m18LRC2**	1644–1660	1660–1676	1644–1660	1660–1676	2×(16+16)
8	m18LRC3	1652–1668	1668–1684	1652–1668	1668–1684	2×(16+16)
9	m18LRS3	1664–1668	1668–1672	1664–1668	1668–1672	2×(4+4)
10	m18R6LC2	4812–4828	4828–4844	1644–1660	1660–1676	2×(16+16)
11	m18R6LC3	4820–4836	4836–4852	1652–1668	1668–1684	2×(16+16)
12	**m18R135LC2**	22212–22228	22228–22244	1644–1660	1660–1676	2×(16+16)
13	m18R135LC3	22220–22236	22236–22252	1652–1668	1668–1684	2×(16+16)
14	**m18L135RC2**	1644–1660	1660–1676	22212–22228	22228–22244	2×(16+16)
15	m18L135RC3	1652–1668	1668–1684	22220–22236	22236–22252	2×(16+16)
16	**m135LRC2**	22212–22228	22228–22244	22212–22228	22228–22244	2×(16+16)
17	m135LRC3	22220–22236	22236–22252	22220–22236	22236–22252	2×(16+16)
18	m135LRS2	22224–22228	22228–22232	22224–22228	22228–22232	2×(4+4)
19	m135LRS3	22232–22236	22236–22240	22232–22236	22236–22240	2×(4+4)
20	m135LRS4	22240–22244	22244–22248	22240–22244	22244–22248	2×(4+4)
21	m135LRSYNC2	22212–22228	22228–22244	Switching frequency		2×(16+16)
22	m135RLSYNC2	Switching frequency		22212–22228	22228–22244	2×(16+16)

in the subsection 4.1.1.

Many combinations of frequency range and polarization are possible for observations with the RadioAstron SRT. In order to simplify proposal composition and subsequent scheduling, we present in Table 3 the most common observing configurations with their corresponding mode name. The table shows the frequency configurations for every mode. Channels 1 and 2 correspond to the two input channels of the Formatter. For the every channel LSB and USB frequency range are presented in the table. Remember, that the LSB spectra are inverted. The last column indicates the total recorded band. Modes that were already used in RadioAstron observations are shown in bold in the table.

Observations in the L-band facilitate limited capability of observing OH Megamaser activity. The LO-2 settings in Table 3 suggest a maximum redshift for extragalactic OH emission of $z = 0.0104$ (3123 km/s).

4.1.1 K-band observing and MFS

The last two observing modes (m135RLSYNC2, m135LRSYNC2) describe the procedure for multi-frequency synthesis (MFS) in the 18 to 25 GHz frequency range. In these modes one polarization channel (RCP or LCP) operates at a fixed frequency, while the second polarization channel switches frequency in steps of 960 MHz starting at the lowest value of 18392 MHz, which corresponds to the 512 MHz IF input of the Formatter. The highest frequency is 25112 MHz. The observing interval is 300 seconds for each of the eight frequencies and the whole cycle takes 40 minutes. The next cycle starts again at the lowest frequency. Table 4 presents results of in-orbit sensetivity measurements for the eight sub-bands of the discussed MFS mode of observations.

Besides these automatic MFS modes, one may select a particular frequency switching or a static configuration by issuing a specific sequence of commands. Below is a simple expression to calculate the possible sky frequency values correspondingly to the center point of USB/LSB band:

$$F_{j,k} = 22232 + 960j + 32k - (512 - F_f),$$

where $j = -4, -3, -2, -1, 0, 1, 2, 3$, $k = 0, -1, -2, -3$, and the F_f are the LO-2 values used in the Formatter (Table 2). The j values select the MFS frequencies, and k provides additional frequency tuning to allow for observations of the extragalactic H_2O Megamaser emission. Thus, the coarse (j) and the fine (k) tuning provide narrow redshift windows of $z = 0.0000 - 0.0053$, $0.0424 - 0.0485$, $0.0855 - 0.0917$, $0.1287 - 0.1348$, and $0.1719 - 0.1780$. **For $j \neq 0$, the parameter k can only be set as $k = 0$. For $j = 0$, one can select the value of k from $k = 0, -1, -2, -3$.**

Table 4: SRT and interferometric sensetivity estimates in the wide K-band.

Sub-Band	Frequency (MHz)	$\mathrm{SEFD_{SRT}}$ (kJy)	$\sigma_{\mathrm{GBT-SRT}}$ (mJy)
F−4	18 392	26	12
F−3	19 352	28	13
F−2	20 312	31	14
F−1	21 272	34	14
F0	22 232	37	15
F1	23 192	41	16
F2	24 152	46	16
F3	25 112	51	17

The one-sigma baseline sensitivity $\sigma_{\mathrm{GBT-SRT}}$ is estimated for the RadioAstron-GBT pair for a 300 s integration time and 16 MHz bandwidth of a single polarization single frequency channel (IF).

4.2 Resolution

The smallest fringe spacing of 7 μas is achieved with the largest ground-space baseline at K-band, see Table 1 for details. The effective resolution of reconstructed space-VLBI images for different types of (u, v)-coverage can be found in Table 7.

4.3 System sensitivity

The parameters of the RadioAstron on-board receiver system have been measured in the laboratory at a physical temperature equivalent to the one expected during space operation, where passive cooling

will give a physical temperature of $t_{LNA} = 130K$. The losses in the cable connections to the feeds were measured separately, as well as losses in the feeds themselves. The T_{sys} values may then be calculated using the following expression:

$$T_{sys} = T_{sky} + t_{dish}(L_{dish} - 1) + t_{feed}L_{dish}(L_{feed} - 1) + t_{cbl}L_{dish}L_{feed}(L_{cbl} - 1) + L_{dish}L_{feed}L_{cbl}T_{LNA},$$

where L_{feed}, L_{cbl}, and L_{dish} are losses in the feed, cable and SRT surface, respectively. The t_{feed}, t_{cbl}, and t_{dish} values are the respective expected physical temperatures in K. Table 5 presents an L values and the expected physical temperatures (t) (in K) for each frequency, where L has been defined as $L = 1/k$ with k being the partial power loss in the corresponding device; for example, for $k = 0.98, L = 1.020$.

Table 6 presents calculated T_{sys} values for the RadioAstron receiver systems and estimates of the expected sensitivity of space-ground interferometry with SRT and using the NRAO GBT telescope as an example ground station. The system equivalent flux density (SEFD) has been calculated as $SEFD = 2kT_{sys}/A_e$. Estimates of the minimum detectable correlated flux density ($\sigma = \frac{1}{\eta_Q}\sqrt{\frac{SEFD_1 SEFD_2}{2\Delta\nu\tau}}$) are made for single polarization frequency channel (IF) with 16-MHz bandwidths and with $\eta_Q = 0.637$ for one bit sampling. The sensitivity for L-, C-, and K-bands channels is improved by a factor of two when both LSB/USB and LCP/RCP channels are combined.

4.4 Experiment preparation

The software package FakeSat, originally developed by David Murphy, has been modified for the RadioAstron mission and re-named FakeRat. FakeRat works under the LINUX operating system and can be used as planning software for potential observer. The required modifications to the FakeSat package included a presentation of the satellite orbit as a table of the state vectors provided by the ballistic center, since a Keplerian orbit treatment does not apply for the Moon-perturbed orbit of RadioAstron. Other modifications concern any operational constraints intrinsic to the RadioAstron spacecraft. The FakeRat package can be obtained at the RadioAstron server together with a *FakeRat User's Guide*. The FakeRat provides all-sky (u, v)-coverage for a given date and a session duration; (u, v)-coverage for a selected source, source visibility from ground radio telescopes, and conditions for communication with the tracking stations.

The link to FakeRat software is: `http://www.asc.rssi.ru/radioastron/software/soft.html` .

4.5 Observing strategy and imaging

4.5.1 All-sky (u,v)-plots

The functional constraints described in section 2.4 restrict available areas on the sky. These areas are presented in Figures 9, 10 as all-sky (u, v)-plots, calculated by FakeRat software for the current version of the orbit predicted for the next several years and tracking stations in Pushchino and Green Bank. The (u, v)-plots are calculated for C-band for a full orbit time interval at the every crossing of the coordinate grid with a step of 20° in declination and two hours in right ascension. In these figures line drawn through "P" (perigee) and "A" (apogee) represents the orbit projection on the sky, and another solid line designates a border separating regions available and forbidden for observations because of constraints related with the Sun position. As was explained in section 2.4 the hemisphere with the Sun at the pole is unavailable for observations; there is also a "blind spot" in the anti-Sun point. The most favorable conditions for observations are during the periods when the Sun is close to the perigee (November–February). Unfavorable circumstances occur when the Sun is close to the

Table 5: The losses L and physical temperatures t of the RadioAstron receiver system as measured in a laboratory

	P-band		L-band		C-band		K-band	
	L	t (K)	L	t (K)	L	t (K)	L	t (K)
Cable	1.040	230	1.036	150	1.058	150	1.000	150
Feed	1.250	170	1.020	170	1.106	170	1.076	170
Dish surface	1.020	200	1.020	200	1.020	200	1.020	200

Table 6: The sensitivity of the RadioAstron mission, in-orbit measurements

	RadioAstron			
	P-band LCP; RCP	L-band LCP; RCP	C-band LCP; RCP	K-band LCP; RCP
BW (MHz)	16; 16	2×16; 2×16	2×16; —	2×16; 2×16
T_{sys}(K)	145±15; 147±15	41.0±4.0; 43.5±4.0	147±8; —	127±8; 100±10
$A_e(m^2)$	30	41	35	7.5
SEFD (kJy)	13.3±1.4; 13.5±1.4	2.76±0.27; 2.93±0.27	11.6±0.63; —	46.7±3.0; 36.8±3.7
	GBT			
T_{sys}(K)	105	20	18	35
$A_e(m^2)$	5500	5500	5500	4800
SEFD (Jy)	55	10	8	23
	RadioAstron–GBT			
1σ ($\tau = 1\,$s)	237; 239	46; 47	85; —	288; 255
1σ ($\tau = 300\,$s)	14; 14	3; 3	5; —	17; 15

Notes: System temperature does not include the background radiation. The 1σ baseline sensitivity is shown for the 16 MHz bandwidth of a single polarization single frequency channel (IF) to be used for detection cutoff estimates. It is recommened to use $S_{\rm cutoff} = 6\sigma$ as a conservative detection cutoff estimate.

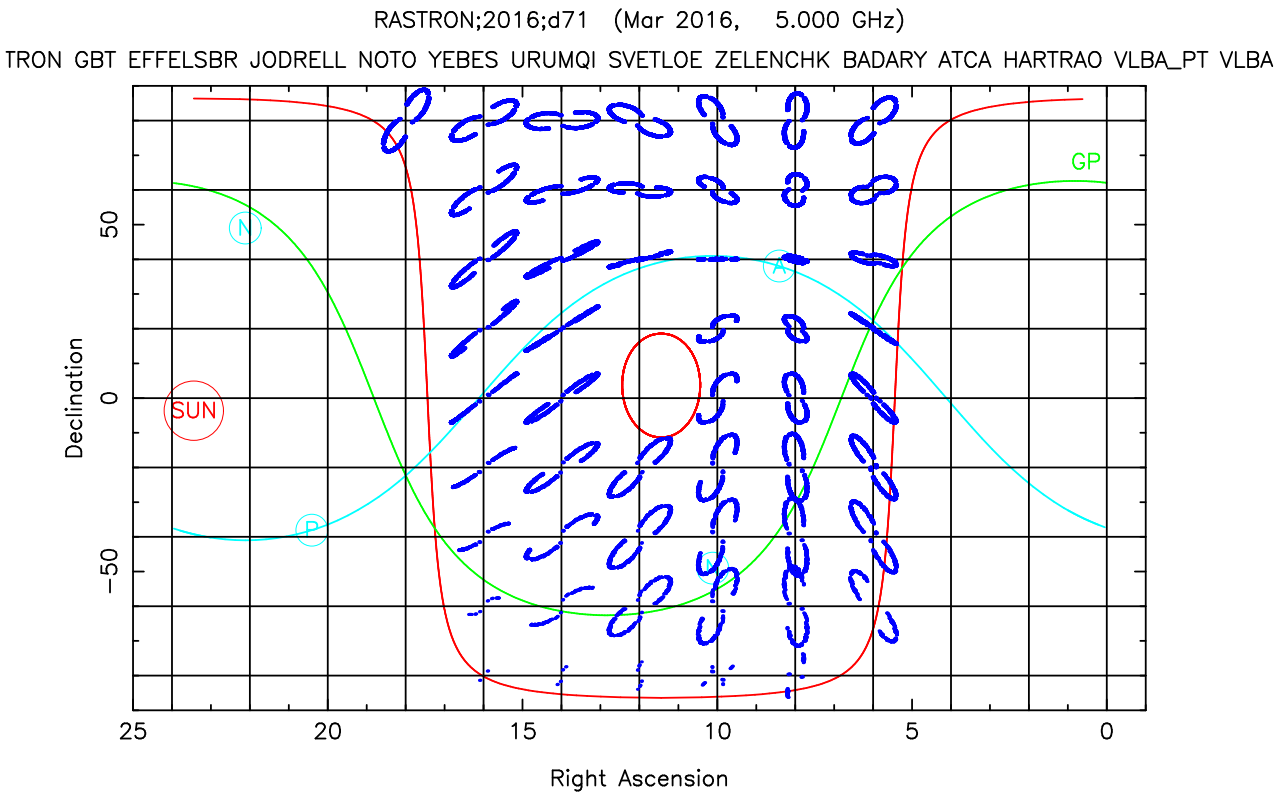

Figure 9: All-sky (u, v)-plots for March 2016. Two operational tracking stations (Pushchino and Green Bank) are used in the calculation. A full orbit has been used for each observation.

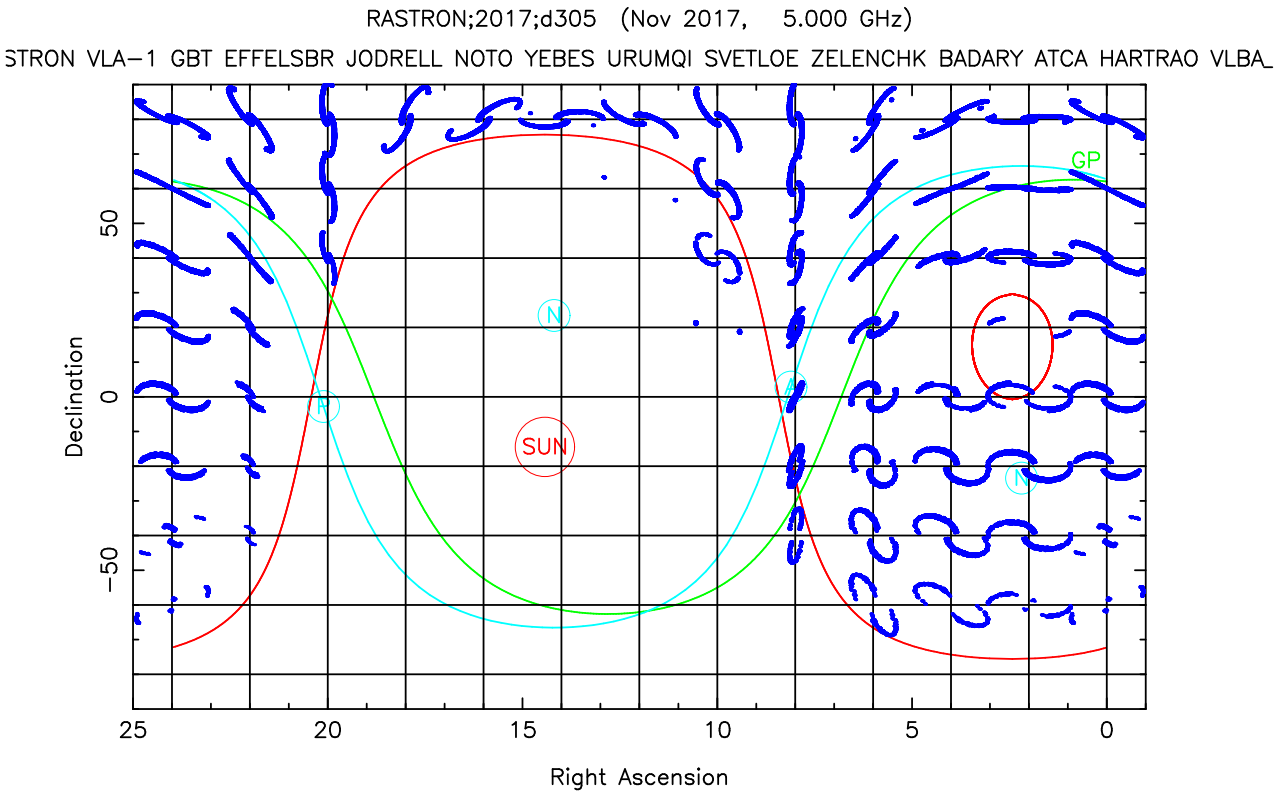

Figure 10: All-sky (u, v)-plots for November 2016. Two operational tracking stations (Pushchino and Green Bank) are used in the calculation. A full orbit has been used for each observation.

apogee (May–August). This is because of constraints connected with the communication antenna, which must be pointed to the tracking station (TS); communication with the TS is impossible when the spacecraft is between the Earth and the Sun in the apogee portion of the orbit.

We note that the mission is currently working together with South Africa on implementing a TS in the Southern hemisphere. This will improve the achievable (u, v)-coverage around perigee.

4.5.2 Examples of observing strategies

In order to implement peculiarities of high-apogee moon-perturbated RadioAstron orbit the mission envisages some typical strategies of the observations: survey at different (u, v)-spacings (e.g., study of brightness temperatures in blazars or pulsar/ISS studies), perigee imaging, near-orbit-plane imaging, apogee imaging, all-orbit synthesis, relative astrometry measurements.

A survey of brightness temperatures can be conducted by observing large sample of AGNs at progressively increasing baseline lengths. Pulsar observations can be done successfully at any baseline projection due to pulsars' extreme compactness but ISS properties can limit the baseline length at which correlation is found. The near-perigee imaging is continuum observations of single radio source during 4–24 hours with the SC passing perigee portion of the orbit. Duration of an observing set will be restricted by the functional and visibility constraints. Space-ground baseline projections will be in the range of 30000 km, thus providing reasonably good (u, v)-coverage. Examples of such (u, v)-coverages are presented in Fig. 11. The near-orbit-plane imaging will be conducted recurrently for several radio sources located close to the orbit plane during SC passing this direction providing relatively short baselines. The observing session will take from 12 to 24 hours because of low speed of the SC. Therefore, during this period several sources may be observed alternatively. The near-apogee imaging would take even longer time of every source (24–48 hours). Such observations may be combined with other measurements, such as survey of brightness temperatures. All-orbit synthesis will be used for prospective bright sources by observing a source during a whole orbit ar even during several orbits. Such observations will be combined with other types of measurements. This strategy is especially useful in MFS frequency mode which reduces the gaps in (u, v)-coverage.

4.5.3 Imaging capabilities

As discussed above, there are three basic modes envisaged for imaging experiments: perigee imaging, apogee imaging and orbital plane imaging. Several typical imaging experiments with RadioAstron are described in Table 7 and Figs. 11–13. In all these experiments, RadioAstron tracking is assumed to be done with a single tracking station in Pushchino only. The experiment 1(P) is a perigee imaging observation, the experiments 2–4(A) are examples of apogee imaging observations and the observation 5(O) is an observation of an object near the orbital plane of RadioAstron. The latter mode allows sampling small spatial frequencies also on baselines to RadioAstron, which will be beneficial for improving the (u, v)-coverage and calibrating space baseline data. Respective (u, v)-coverage and histograms of visibility distributions are shown in Figs. 11 and 13.

The effect of the individual (u, v)-coverage on imaging is estimated by the (u, v)-gap parameter, $\Delta u/u$, calculated as a normalized difference $(u_2 - u_1)/u_2$ for any two visibility points within a sufficiently small angular sector (the sector size can be set by the scan length of an observation, with the latter assumed to be 5 minutes, in the examples discussed here). Azimuthal averages of $\Delta u/u$ are shown in Fig 12 for a range of (u, v)-radii. Overall averages of the (u, v)-gap parameter are given in Table 7 and used for deriving the effect of RadioAstron (u, v)-coverage on the image noise and spatial dynamic range (defined as a ratio of largest and smallest structures that can be imaged).

Table 7: Image parameters of selected RadioAstron experiments

Exp.	$t_{\rm obs}$ (hrs)	δ (°)	Ground Telescopes	Beam (μas×μas,°)	$\langle\Delta u/u\rangle$	$\langle\sigma_{\rm uv}\rangle$ ($\sigma_{\rm rms}$)	SDR$_{\rm uv}$ (SDR$_{\rm FOV}$)
(1)	(2)	(3)	(4)	(5)	(6)	(7)	(8)
1 (P)	5	+30°	EbGbJbNbRoUsEv	184×92,+37°	0.25	18.0	0.58
2 (A)	28	+40°	EbGbJbNbY27RoUsEvTb	94×24,+152°	0.09	8.3	0.83
3 (A)	28	+80°	EbGbJbNbY27RoUsEv	80×25,+156°	0.05	4.9	0.90
4 (A)	24	+20°	EbGbJbNbY27RoUsEvTb	156×22,+101°	0.11	5.6	0.82
5 (O)	48	+45°	EbGbJbNbY27RoUsEv	290×89,+54°	0.04	3.0	0.91

Notes: (1) – Experiment code: numbers refer to plot panels in Figs. 11, 12 & 13; letters denote observations near the perigee (P), the apogee (A), and the orbital plane (O); (2) – observation duration (hrs); (3) – declination of the target source; (4) – participating ground telescopes; (5) – estimated beam for uniformly weighted data; (6) – average (u, v)-gap parameter; (7) – noise contribution from incomplete (u, v)-coverage, normalized to the r.m.s. noise; (8) – structural dynamic range (range of structural scales that can be imaged), normalized to the full SDR$_{\rm FOV}$ given the ratio of primary beam of the largest radio telescope participating in an observation to restoring beam of the interferometry data.

The examples described above indicate that the best imaging performance will be achieved with long observations that sample a larger range of spatial frequencies and provide a better chance for inter-calibrating ground and space baselines.

4.6 Post-correlation data processing

The Astro Space Center has developed a software package ASC Locator[6] which can be used for RadioAstron post-correlation data prcoessing. It is also possible to utilize AIPS[7] with its space-VLBI extension and PIMA[8] for the purpose of RadioAstron data processing. The ASC, DiFX, and SFXC software correlators provide results in the FITS-IDI format which is readable by AIPS and PIMA.

[6] `http://asc-lebedev.ru/index2.php?engdep=6&engpage=2`
[7] `http://www.aips.nrao.edu/index.shtml`
[8] `http://astrogeo.org/pima/`

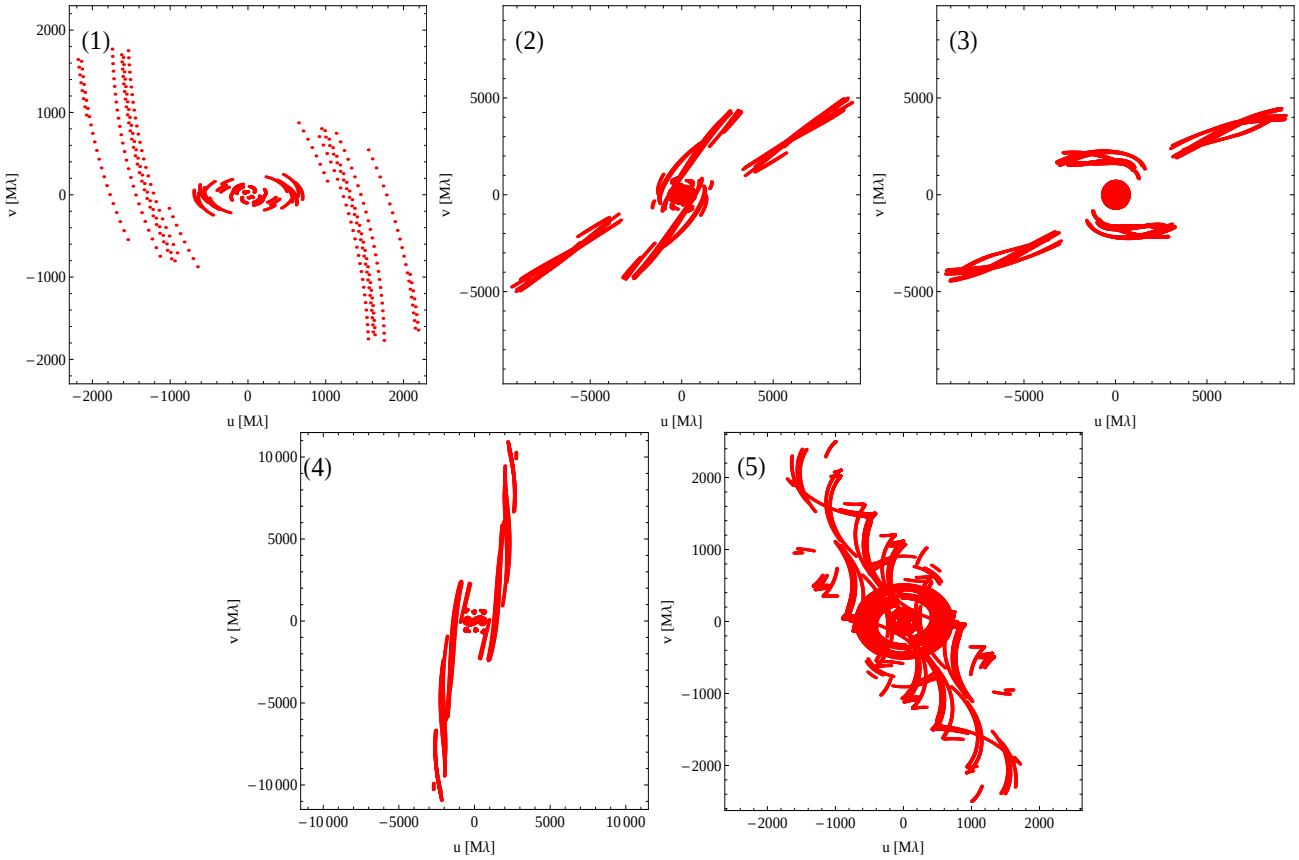

Figure 11: Coverages of the (u, v)-plane for the five experiments listed in Table 7.

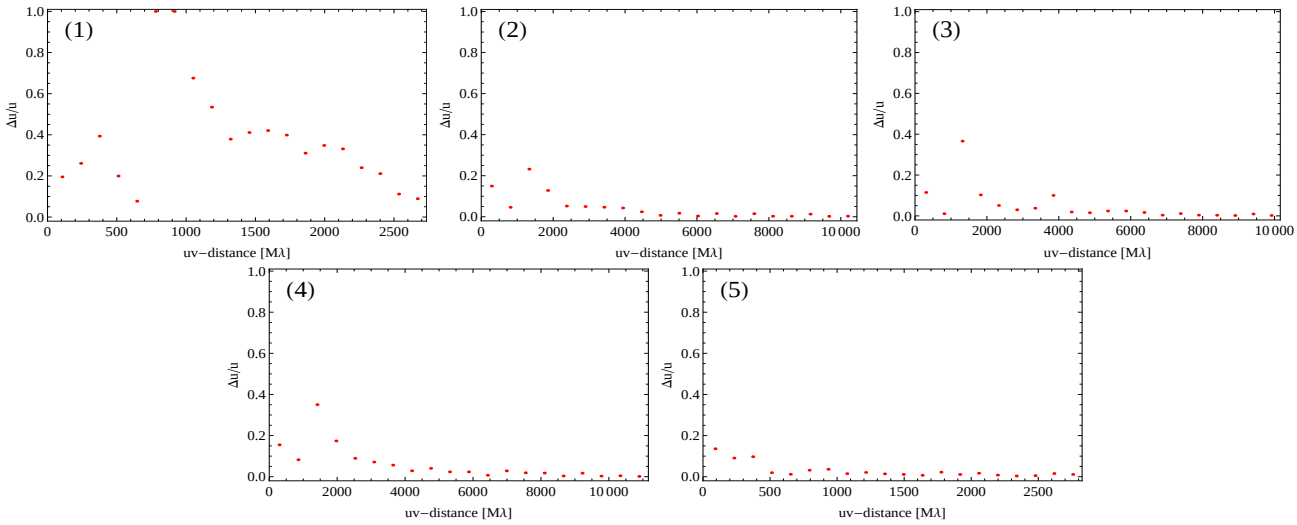

Figure 12: Radial averages of the (u, v)-gap parameter, $\Delta u/u$, for the five experiments listed in Table 7.

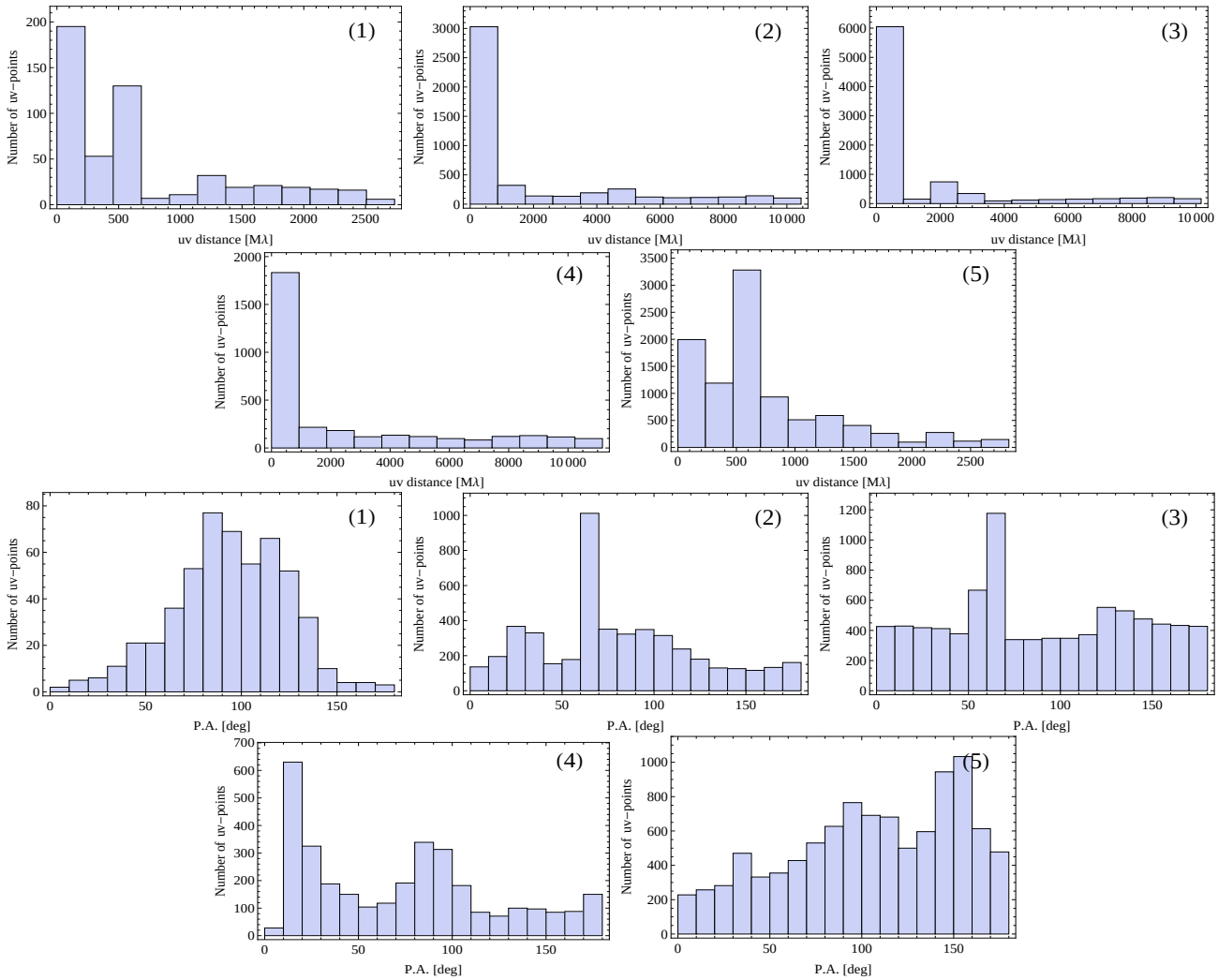

Figure 13: Radial (top two rows) and angular (bottom two rows) distributions of the visibility measurements for the five experiments listed in Table 7.

A Document abbreviations

ADC	Analog-to-Digital Converter
AE	Autonomous Electronics
AO	Announcement of Opportunity
ASC	Astro Space Center
ATCA	Australia Telescope Compact Array
CCW	Control Code Words
CS	Control System
CTS	Command & Telemetry Station
CUFC	Control Unit of the Focal Container
CUIM	Control Unit of the Instrumentation Module
DAS	Data Acquisition System
ESA	European Space Agency
ESP	Early Science Program
ESPT	Early Science Program Team
EVN	European VLBI Network
GBES	Green Bank Earth Station
GOCG	General Operation Control Group
HDRC	High Data Rate Communication radio link (or VIRK)
HEMT	High Electron Mobility Transistor
HFS	High-Frequency Synthesizer
HGCA	High-Gain Communication Antenna
IOC	In-Orbit Checkout
ISAS	Institute of Space and Astronautical Science
JAXA	Japan Aerospace Exploration Agency
KSP	Key Science Program
LA	Lavochkin Association
LCP	Left-hand Circular Polarization
LFS	Low-Frequency Synthesizer
LNA	Low-Noise Amplifier
LO	Local Oscillator
LSB	Lower Side Band
LTS	Long Term Schedule
MFS	Multi-Frequency Synthesis
OCMS	Onboard Command and Measuring System
NAIC	National Astronomy and Ionospheric Center
NCRA	National Centre for Radio Astrophysics
NRAO	National Radio Astronomy Observatory
OCE	Orbit Correction Engines
OCS	Onboard Control System
OM	Orbit Measurements
PRAO	Pushchino Radio Astronomical Observatory
PSS	Power Supply System
PUTS	Pushchino Tracking Station
QPSK	Quadrature Phase Shift Keying
RAM	Random Access Memory device
ROM	Read-Only Memory
RCP	Right-hand Circular Polarization
RDR	RadioAstron Data Recorder

RMST	RadioAstron Mission Scheduling Team
RWS	Reaction Wheel System
SC	Spacecraft
SEFD	System Equivalent Flux Density
SFS	System of Frequency Synthesis
SFXC	EVN software correlator at JIVE
SPAS	Solar Panel Onboard Control System
SRS	File format of LTS and STS
SRT	Space Radio Telescope
STS	Short Term Schedule
TCS	Thermal Control System
TM	Telemetry activity
TMAFS	TM-Antennas and Feeds System
TMS	Telemetry System
TPS	Time-Program System
TS	Tracking Station
UDPTR	Up-Down Phase Transfer Radio link
USB	Upper Side Band
WG	Working Group

B Abbreviations used in the Diagrams

BRC	Backbone Radio Complex
CU DP	Control Unit of the Device Package
CU FP	Control Unit of the Focal Package
DC-DC HF C conv.	Power Supply of the C-band Receiver and Low-Noise Amplifier [C]
DC-DC HF L conv.	Power Supply of the L-band Receiver and Low-Noise Amplifier [L]
DC-DC HF/M conv.	Power Supply of the K-band Receiver and Low-Noise Amplifier
DP	Device Package (The Instrumental Module)
FA	Feeding Antenna
FP	Focal Package (The Focal Container)
FU	Focal Unit (The Feed Module)
HCFS	Heterodyne and Clock Frequency Synthesizer
HRIRC	High Rate Information Radio Complex
IF Selector	Intermediate Frequency Selector
IF	Intermediate Frequency
LNA-1.35 cm	K-band Low Noise Amplifier
LNA-18 cm	L-band Low-Noise Amplifier
LNA-6 cm	C-band Low-Noise Amplifier
OFFS-SRT	Space Radio Telescope On-board Frequency Forming System
OHCFS	On-board Heterodyne and Clock Frequency Synthesizer
OHCFS-SRT	Space Radio Telescope On-board Heterodyne and Clock Frequency Synthesizer set
OHFS-SRT	Space Radio Telescope On-board Hydrogen Frequency Standard
ORFS-SRT	Space Radio Telescope On-board Rubidium Frequency
OUHFS	On-board Ultra high Heterodyne Frequency Synthesizer Standard
PCS	Pulse Calibration System
PS HCFS	Power Supply of the Heterodyne and Clock Frequency Synthesizer
RF	Reference Frequency

RFS	Space Radio Telescope On-board Rubidium Frequency Standard
R-SRT-1.35 cm	K-band Receiver
R-SRT-92 cm	P-band Receiver
SHM	Space H-Maser
SRT-18 cm	L-band Low-Noise Amplifier
SRT-6 cm	C-band Receiver
TRM	TRansMitter of the High Rate Information Radio Complex
TRP	TRansPonder of the High Rate Information Radio Complex
UHFS	Ultra high Heterodyne Frequency Synthesizer
VDC-SRT	Control Video Digital Converter (Formatter)